# Study of $\chi_{cJ}(J = 0, 1, 2) \rightarrow p\bar{p}\eta\pi^0$ and $\psi(2S) \rightarrow \Lambda(1520)\bar{\Sigma}^0\eta(\pi^0) + c.c.$

**Speaker: Wenpeng Yan**

**HTU Group Meeting, Mar.5th, 2024**

# Analysis I: Intermediate state investigation

**Re: Memo is ready for you review**

发起会议
2024-01-11 19:31:17

发件人： "Wolfgang Kuehn" <W.Kuehn@physik.uni-giessen.de>

收件人： "闫文鹏" <yanwp@ihep.ac.cn>

抄 送： "jiqingping@htu.edu.cn" <jiqingping@htu.edu.cn> "WANG Zhiyong" <wangzy@ihep.ac.cn> "Kai Zhu" <zhuk@ihep.ac.cn> "Yuping" <guoyp@fudan.edu.cn>

Dear Authors,

thank you for preparing this interesting memo.

Here are my comments and suggestions:

Table 8: "Pollution" and "Misjudgement Rate" aren't well defined concepts and should not be used without precise definition in a scientific document.

Fig. 9 ff. The Dalitz plots show strong evidence for all kinds of intermediate states, both in the meson and the baryon sector. In view of that observation, reporting just an integrated $\chi cJ \to p\bar{p}\eta\pi 0$ rate is only of limited use, at least for any theorist who would like to understand the data.

You should make an attempt to extract at least the strongest intermediate channels and report their branching fractions in the summary. I realize, however, that this is not trivial due to the possible presence of interference effects.

The importance of the intermediate states is further corroborated by the strong disagreement between data and MC shown in fig. 16. Have you tried to improve the agreement by adding some of the strongest channels to the signal MC?

Best regards,
Wolfgang

# Analysis I: Intermediate state investigation

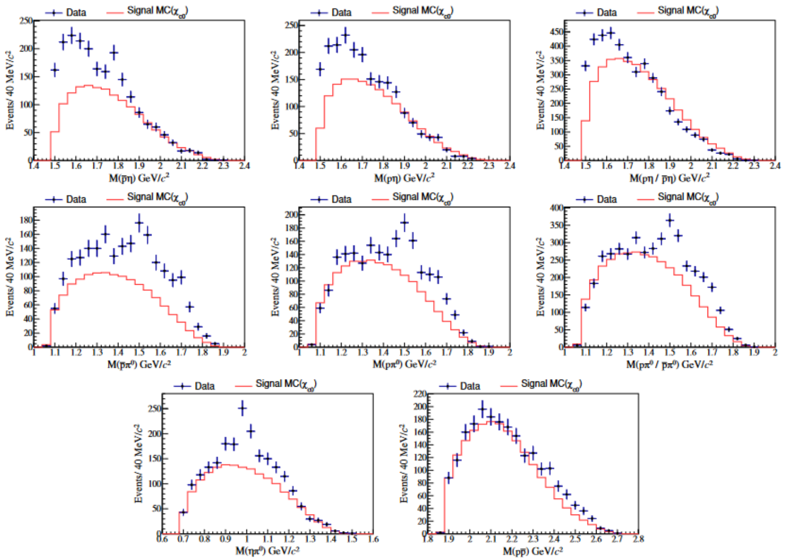

$\chi_{c0}$ region

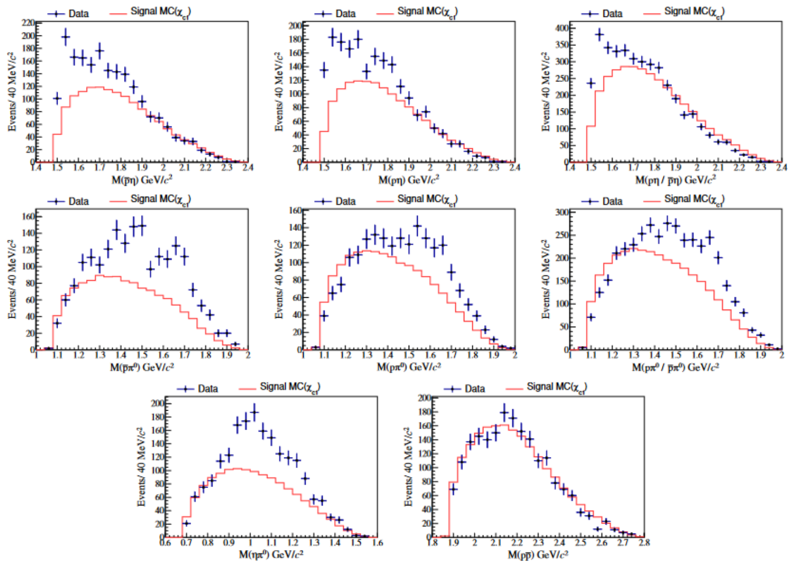

$\chi_{c1}$ region

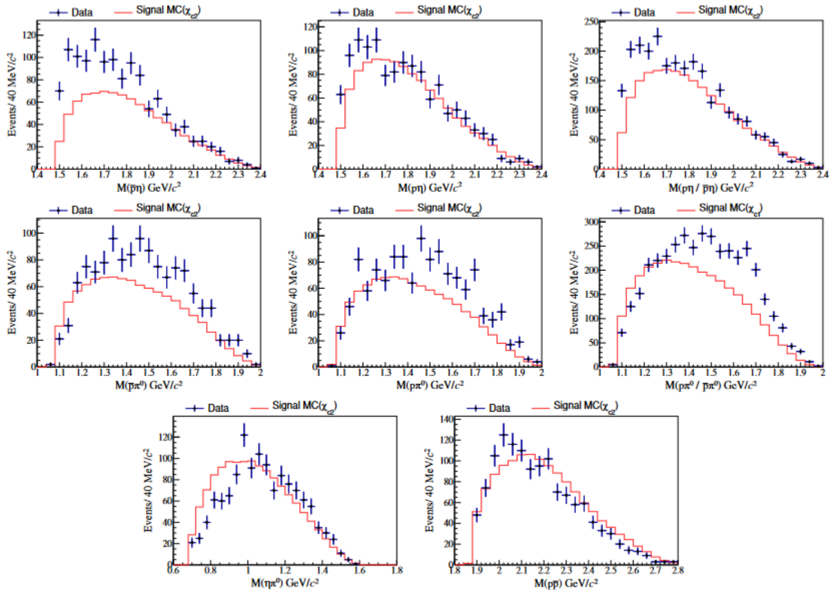

$\chi_{c2}$ region

# Analysis I: Intermediate state investigation

① $\chi_{cJ} \to p\bar{p}a_0(980)$

② $\chi_{cJ} \to N(1535)\bar{N}(1535), N(1535) \to p\eta, \bar{N}(1535) \to \bar{p}\pi^0$
③ $\chi_{cJ} \to \bar{p}\pi^0 N(1535), N(1535) \to p\eta$
④ $\chi_{cJ} \to p\eta\bar{N}(1535), \bar{N}(1535) \to \bar{p}\pi^0$

⑤ $\chi_{cJ} \to N(1535)\bar{N}(1535), N(1535) \to p\pi^0, \bar{N}(1535) \to \bar{p}\eta$
⑥ $\chi_{cJ} \to p\pi^0\bar{N}(1535), \bar{N}(1535) \to \bar{p}\eta$
⑦ $\chi_{cJ} \to \bar{p}\eta N(1535), N(1535) \to p\pi^0$

| | $\chi_{c0}(\%)$ | $\chi_{c1}(\%)$ | $\chi_{c2}(\%)$ |
|---|---|---|---|
| $\chi_{cJ} \to p\bar{p}\eta\pi^0$ | 7.4 | 8.4 | 8.0 |
| $\chi_{cJ} \to p\bar{p}a_0(980), a_0(980) \to \eta\pi^0$ | 7.6 | 8.5 | 8.1 |
| $\chi_{cJ} \to \bar{p}\pi^0 N(1535), N(1535) \to p\eta$ | 7.7 | 8.5 | 8.0 |
| $\chi_{cJ} \to p\pi^0 \bar{N}(1535), \bar{N}(1535) \to \bar{p}\eta$ | 7.5 | 8.4 | 7.9 |
| $\chi_{cJ} \to p\eta\bar{N}(1535), \bar{N}(1535) \to \bar{p}\pi^0$ | 7.9 | 8.5 | 8.0 |
| $\chi_{cJ} \to \bar{p}\eta N(1535), N(1535) \to p\pi^0$ | 7.7 | 8.4 | 7.9 |
| $\chi_{cJ} \to N(1535)\bar{N}(1535), N(1535) \to p\pi^0, \bar{N}(1535) \to \bar{p}\eta$ | 7.8 | 8.7 | 8.1 |
| $\chi_{cJ} \to N(1535)\bar{N}(1535), N(1535) \to p\eta\bar{N}(1535) \to \bar{p}\pi^0$ | 8.1 | 8.9 | 8.7 |

# Analysis I: Intermediate state investigation

**$\chi_{c0}$ region**

① $\chi_{cJ} \to p\bar{p}a_0(980)$

② $\chi_{cJ} \to N(1535)\bar{N}(1535), N(1535) \to p\eta, \bar{N}(1535) \to \bar{p}\pi^0$

③ $\chi_{cJ} \to \bar{p}\pi^0 N(1535), N(1535) \to p\eta$

④ $\chi_{cJ} \to p\eta\bar{N}(1535), \bar{N}(1535) \to \bar{p}\pi^0$

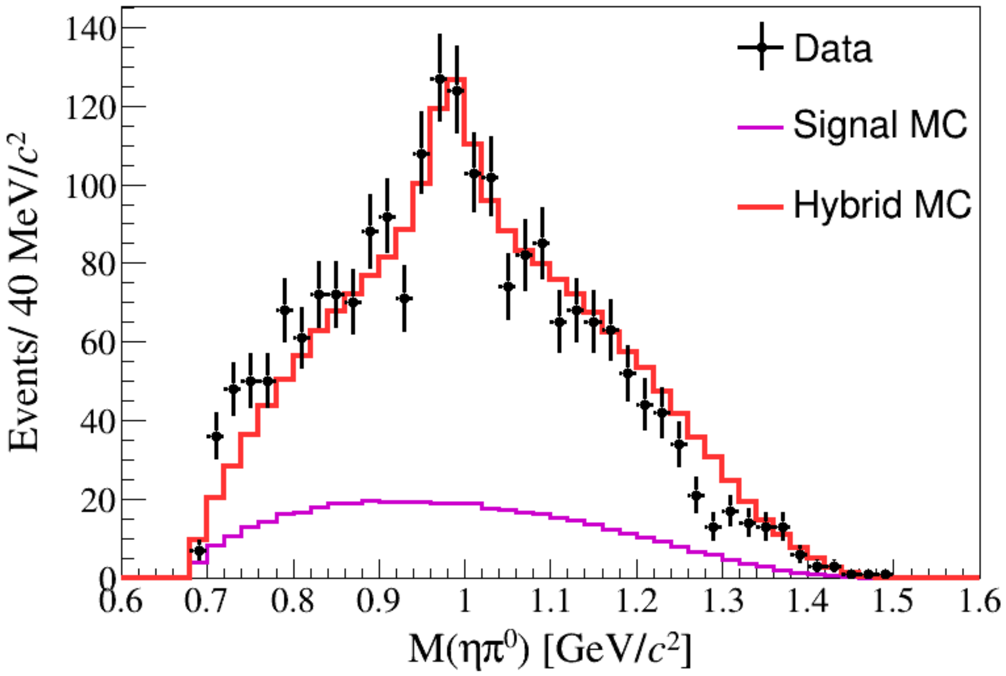


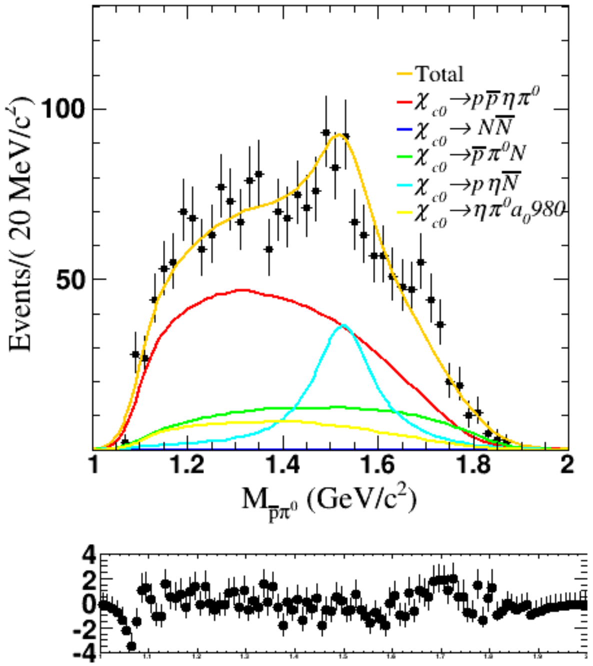


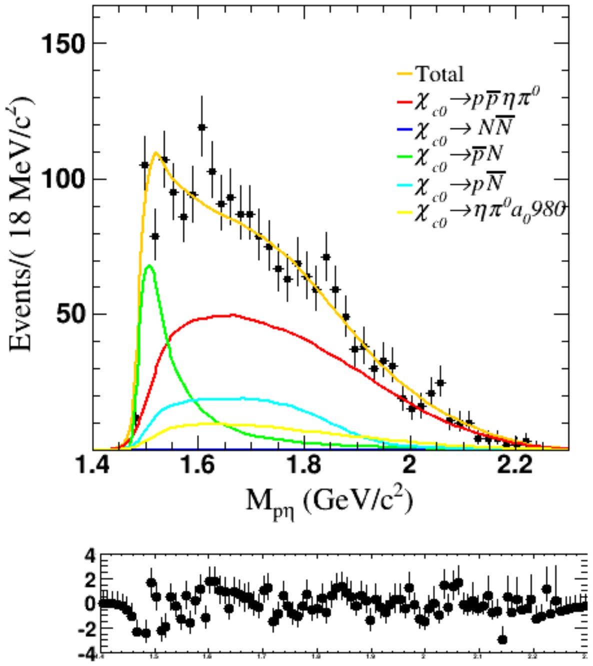

# Analysis I: Intermediate state investigation

$①\ \chi_{cJ} \to p\bar{p}a_0(980)$

$\chi_{c0}$ region

$⑤\ \chi_{cJ} \to N(1535)\bar{N}(1535), N(1535) \to p\pi^0, \bar{N}(1535) \to \bar{p}\eta$

$⑥\ \chi_{cJ} \to p\pi^0\bar{N}(1535), \bar{N}(1535) \to \bar{p}\eta$

$⑦\ \chi_{cJ} \to \bar{p}\eta N(1535), N(1535) \to p\pi^0$

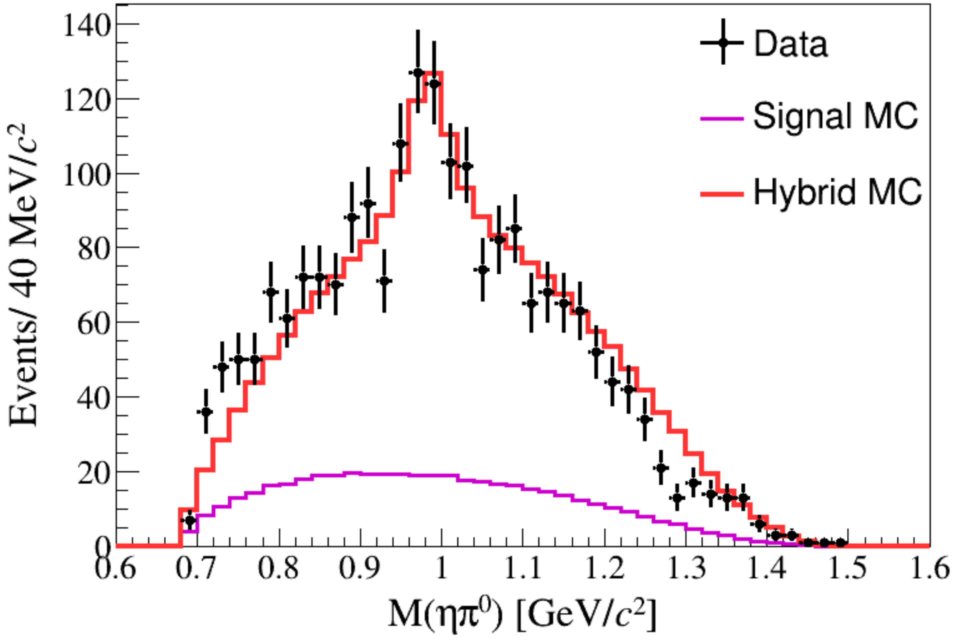


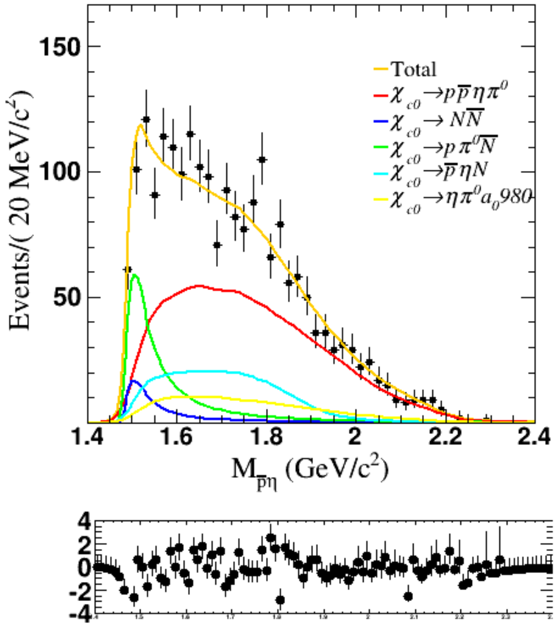


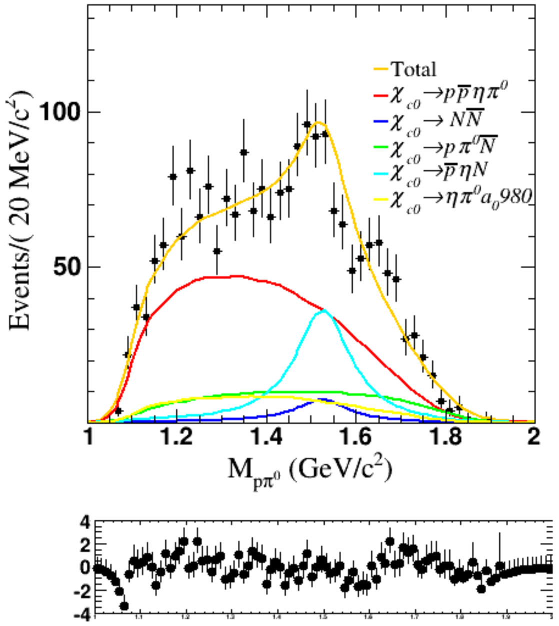

# Analysis I: Intermediate state investigation

## $\chi_{c0}$ region

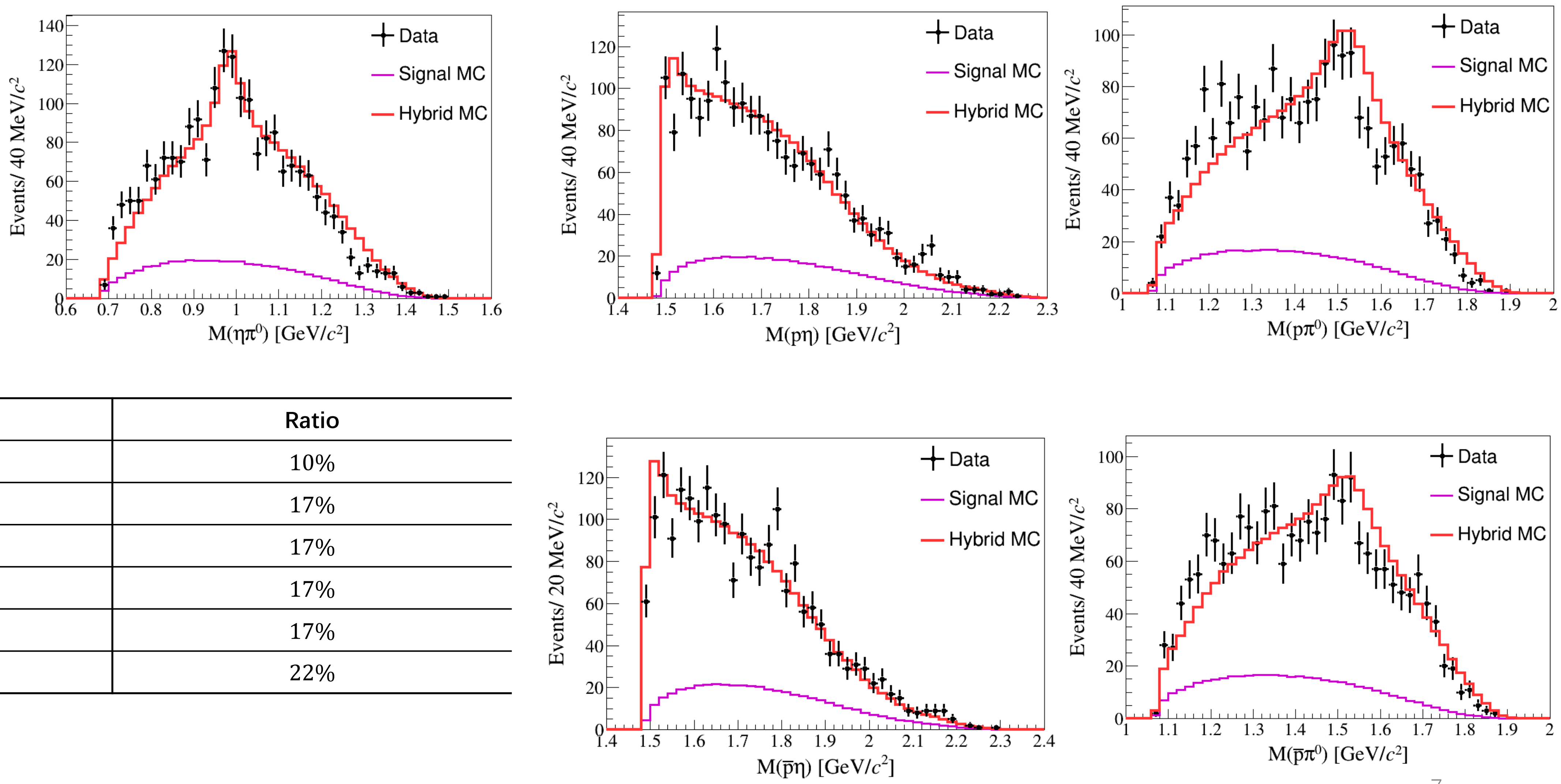


| Decay Chanel | Ratio |
|---|---|
| $\chi_{c0} \to p\bar{p}a_0(980)$ | 10% |
| $\chi_{c0} \to \bar{p}\pi^0 N$ | 17% |
| $\chi_{c0} \to p\eta\bar{N}$ | 17% |
| $\chi_{c0} \to p\pi^0\bar{N}$ | 17% |
| $\chi_{c0} \to \bar{p}\eta N$ | 17% |
| $\chi_{c0} \to p\bar{p}\eta\pi^0$ | 22% |

# Analysis I: Intermediate state investigation

① $\chi_{cJ} \to p\bar{p}a_0(980)$

$\chi_{c1}$ region

② $\chi_{cJ} \to N(1535)\bar{N}(1535), N(1535) \to p\eta, \bar{N}(1535) \to \bar{p}\pi^0$

③ $\chi_{cJ} \to \bar{p}\pi^0 N(1535), N(1535) \to p\eta$

④ $\chi_{cJ} \to p\eta\bar{N}(1535), \bar{N}(1535) \to \bar{p}\pi^0$

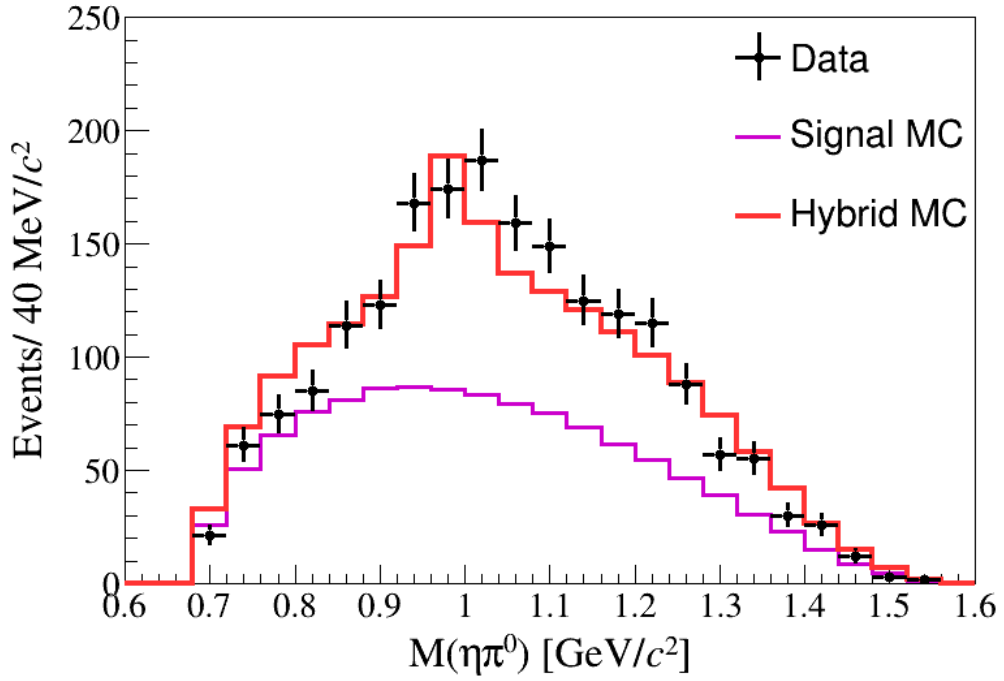


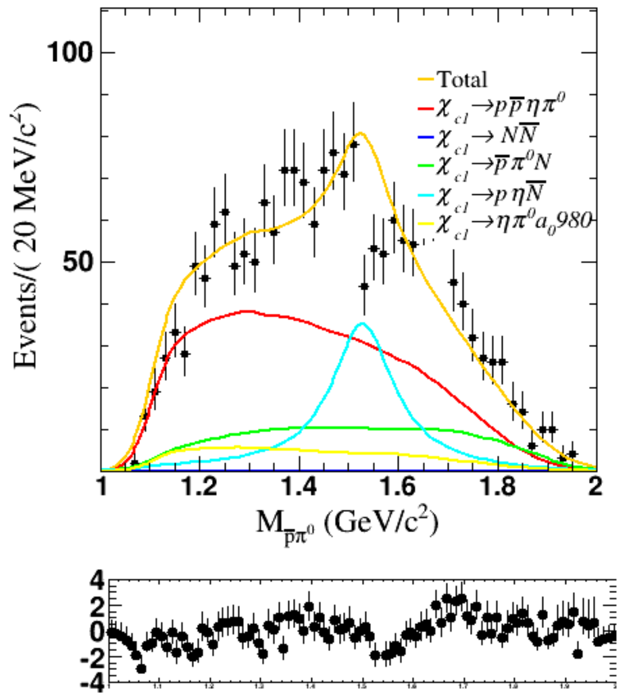


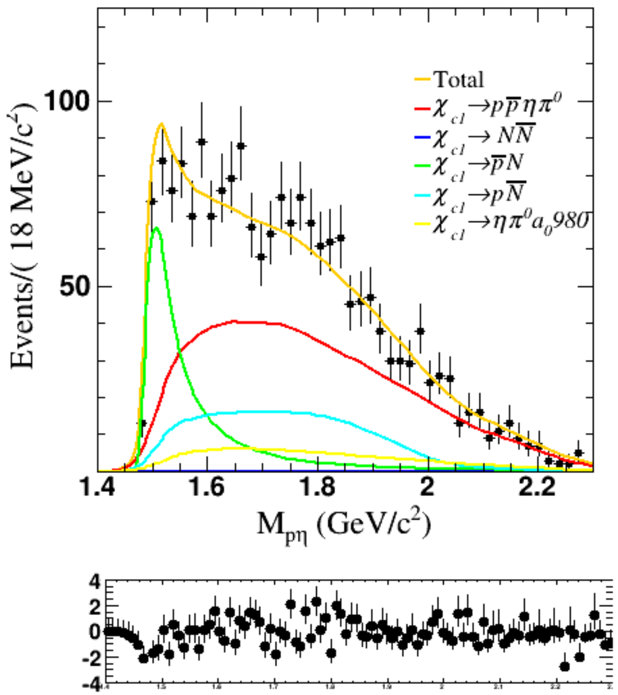

# Analysis I: Intermediate state investigation

$\chi_{c1}$ region

① $\chi_{cJ} \rightarrow p\bar{p}a_0(980)$

⑤ $\chi_{cJ} \rightarrow N(1535)\bar{N}(1535), N(1535) \rightarrow p\pi^0, \bar{N}(1535) \rightarrow \bar{p}\eta$

⑥ $\chi_{cJ} \rightarrow p\pi^0\bar{N}(1535), \bar{N}(1535) \rightarrow \bar{p}\eta$

⑦ $\chi_{cJ} \rightarrow \bar{p}\eta N(1535), N(1535) \rightarrow p\pi^0$

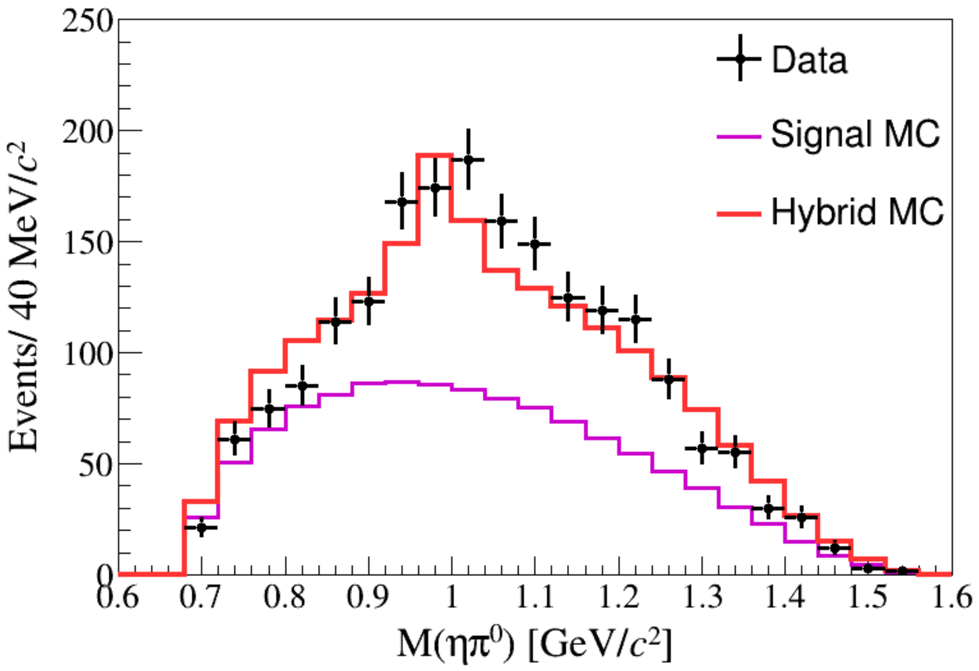


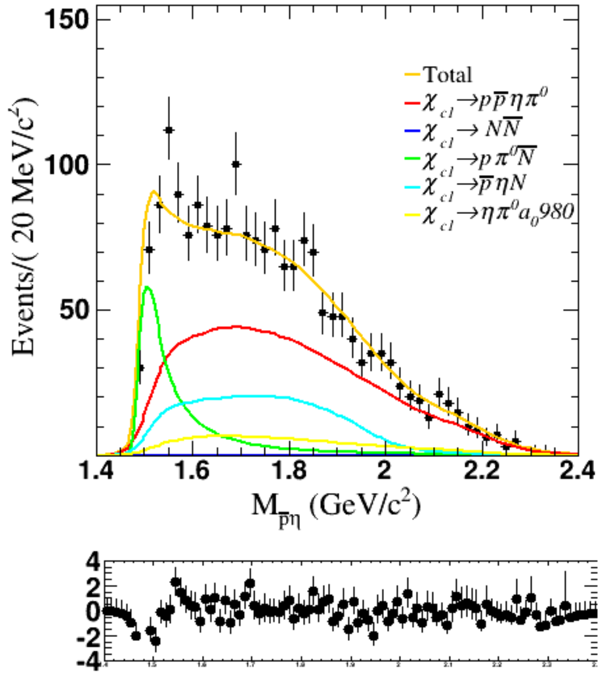


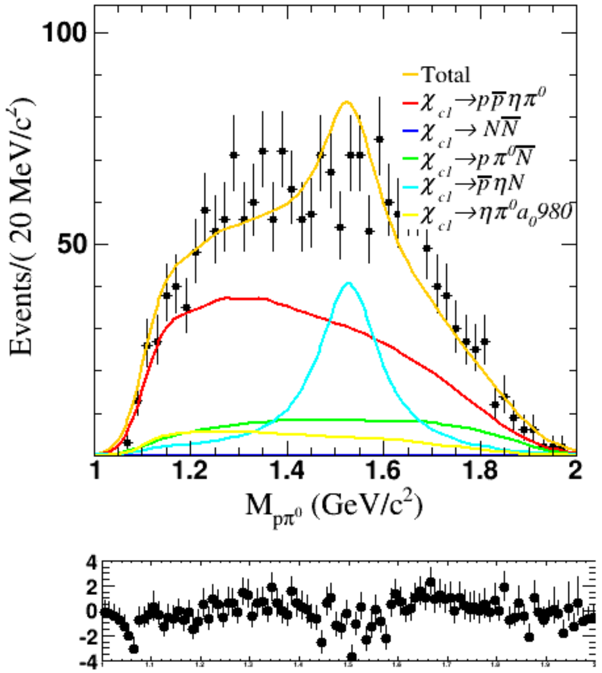

# Analysis I: Intermediate state investigation

## $\chi_{c1}$ region

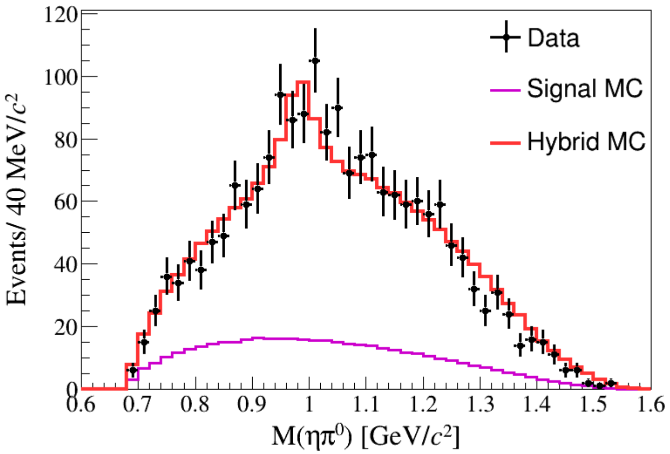


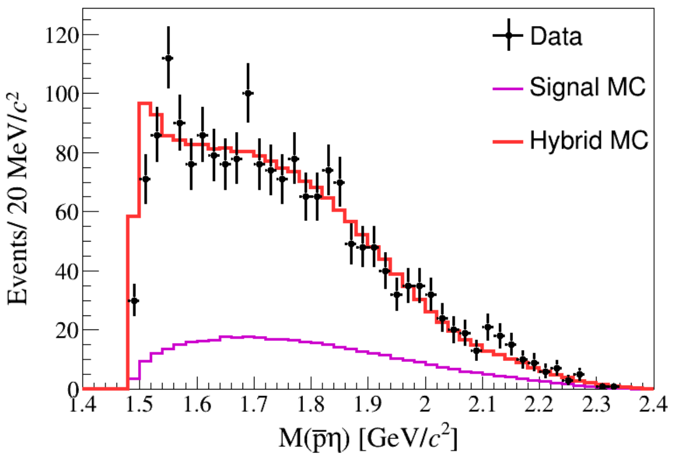


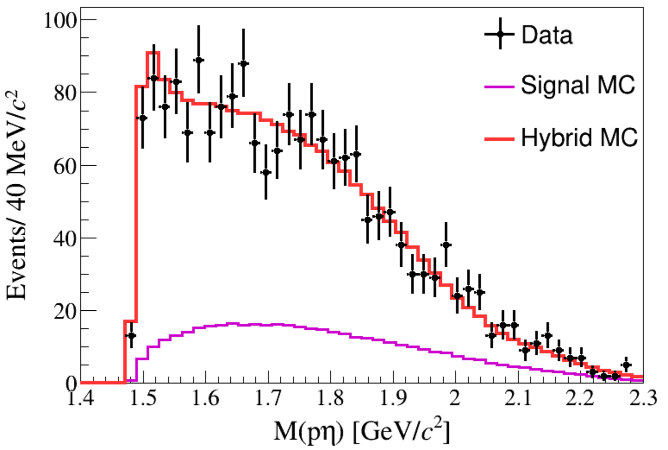


| Decay Chanel | Ratio |
|---|---|
| $\chi_{c1} \to p\bar{p}a_0(980)$ | 8% |
| $\chi_{c1} \to \bar{p}\pi^0 N$ | 15% |
| $\chi_{c1} \to p\eta\bar{N}$ | 20% |
| $\chi_{c1} \to p\pi^0\bar{N}$ | 15% |
| $\chi_{c1} \to \bar{p}\eta N$ | 20% |
| $\chi_{c1} \to p\bar{p}\eta\pi^0$ | 22% |

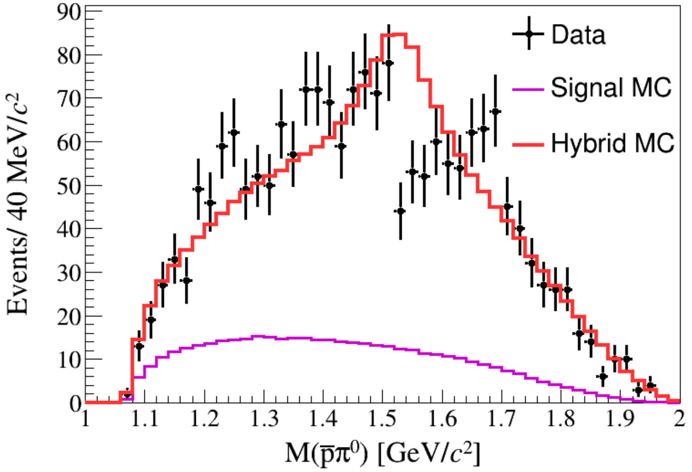


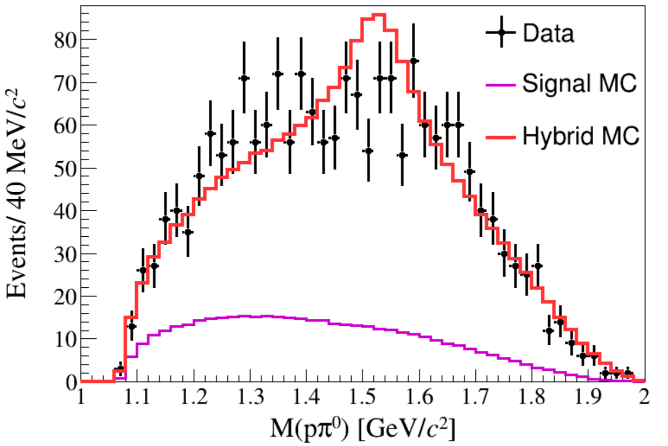

# Analysis I: Intermediate state investigation

$\chi_{c2}$ **region**

① $\chi_{cJ} \to p\bar{p}a_0(980)$

② $\chi_{cJ} \to N(1535)\bar{N}(1535), N(1535) \to p\eta, \bar{N}(1535) \to \bar{p}\pi^0$

③ $\chi_{cJ} \to \bar{p}\pi^0 N(1535), N(1535) \to p\eta$

④ $\chi_{cJ} \to p\eta\bar{N}(1535), \bar{N}(1535) \to \bar{p}\pi^0$

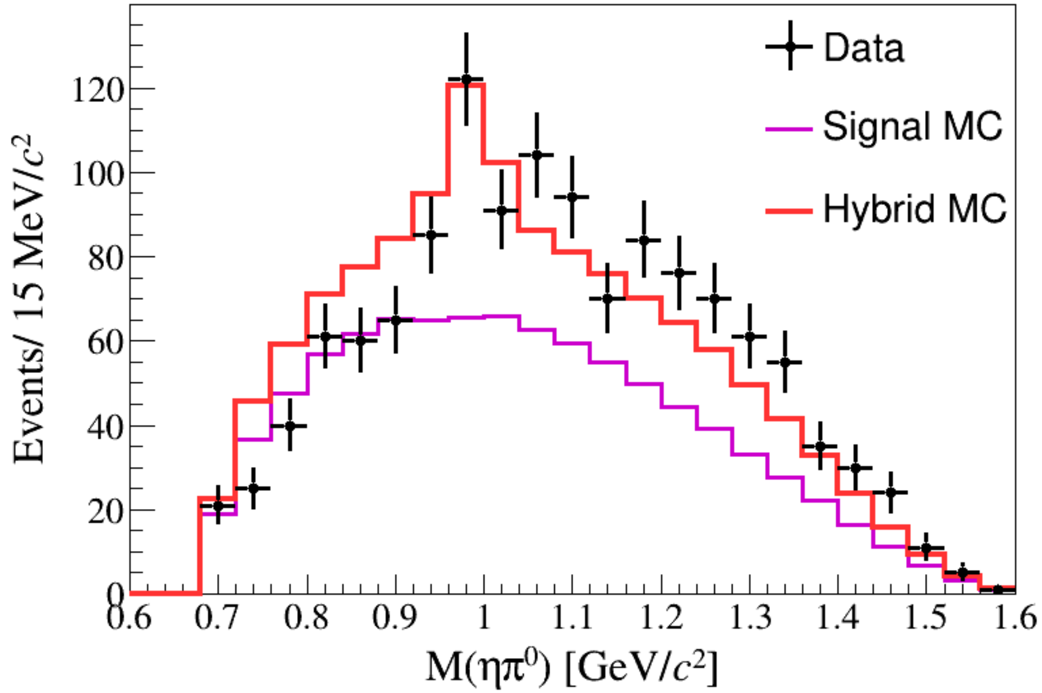


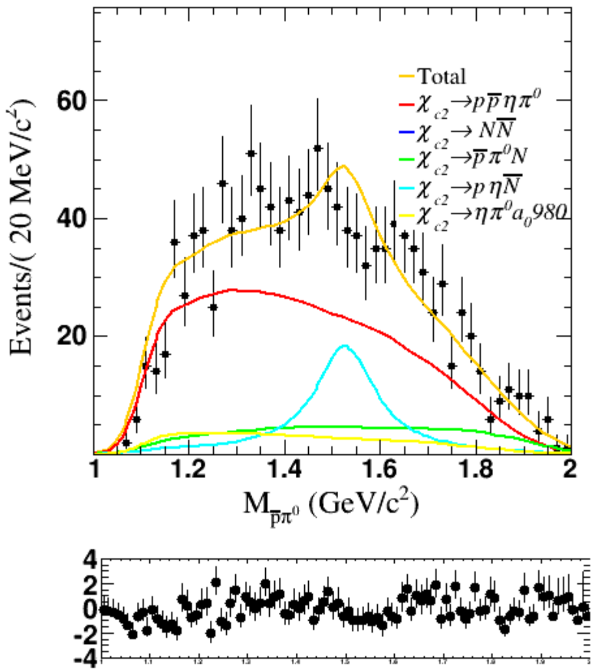


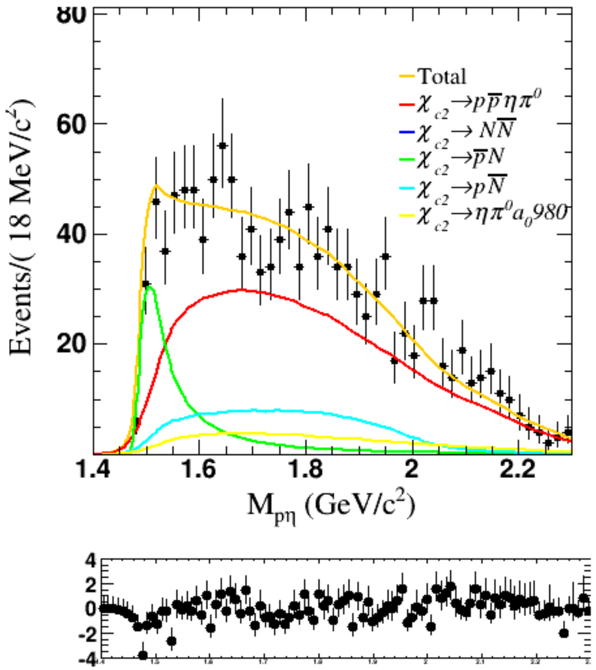

# Analysis I: Intermediate state investigation

① $\chi_{cJ} \to p\bar{p}a_0(980)$

$\chi_{c2}$ **region**

⑤ $\chi_{cJ} \to N(1535)\bar{N}(1535), N(1535) \to p\pi^0, \bar{N}(1535) \to \bar{p}\eta$

⑥ $\chi_{cJ} \to p\pi^0\bar{N}(1535), \bar{N}(1535) \to \bar{p}\eta$

⑦ $\chi_{cJ} \to \bar{p}\eta N(1535), N(1535) \to p\pi^0$

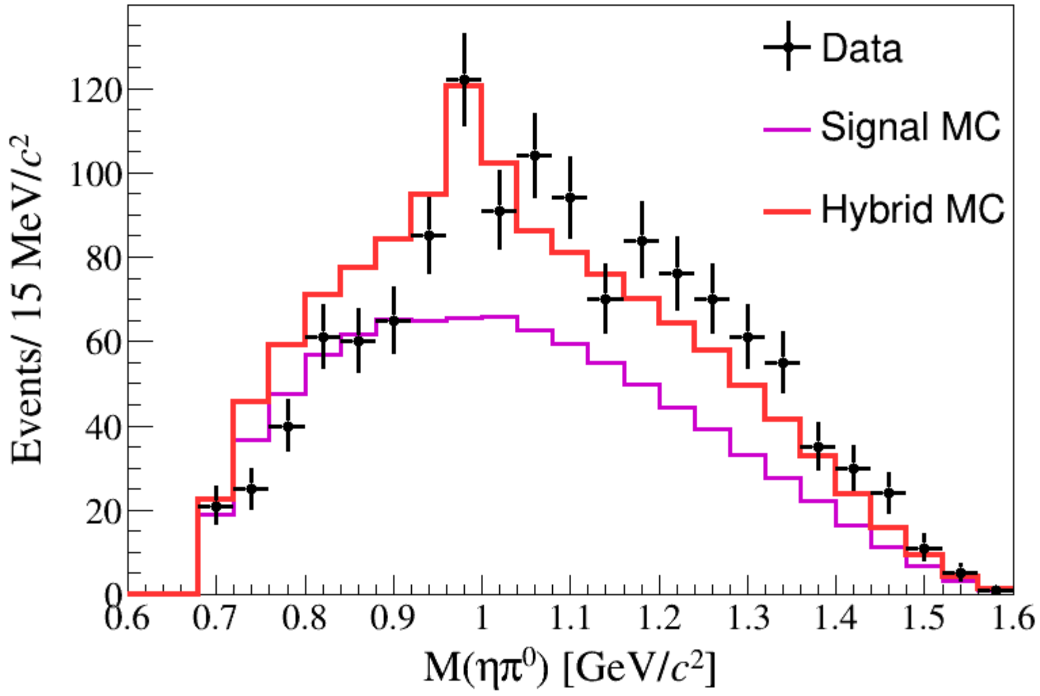


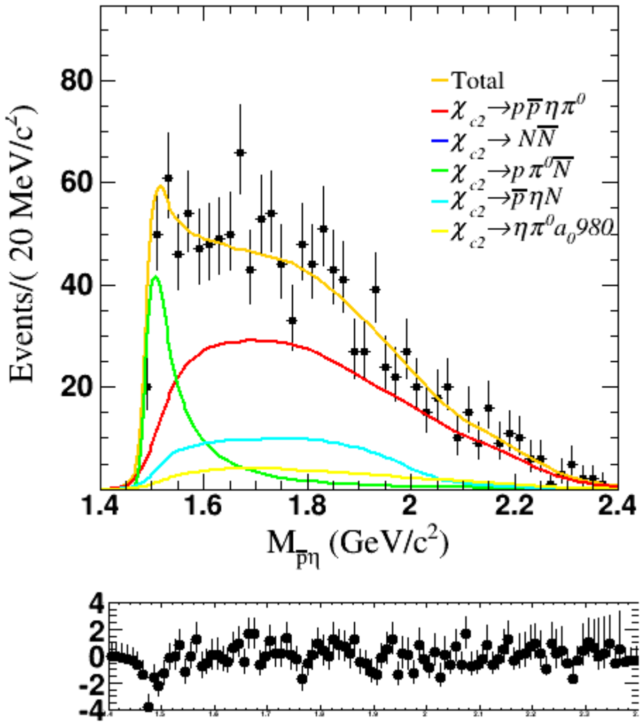


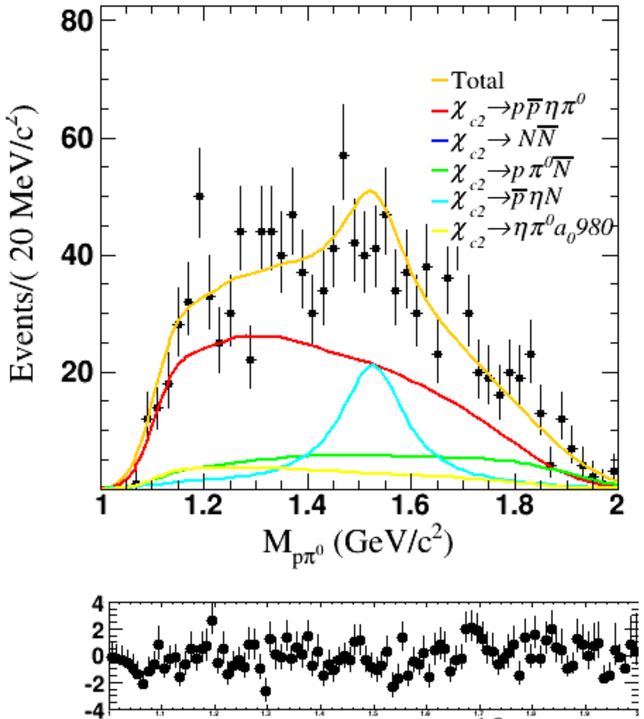

# Analysis I: Intermediate state investigation

## $\chi_{c2}$ region

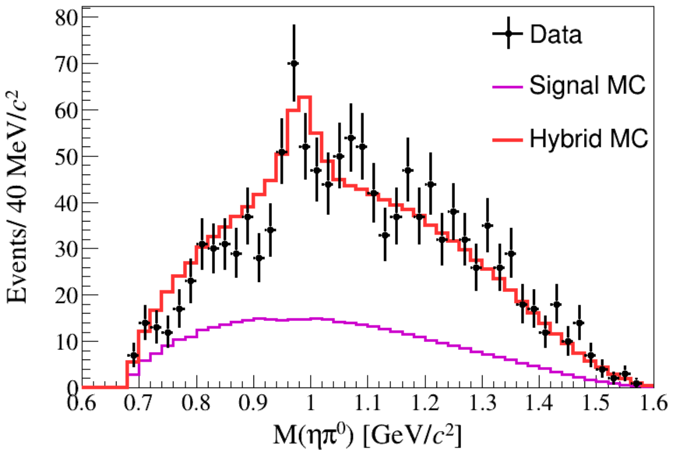


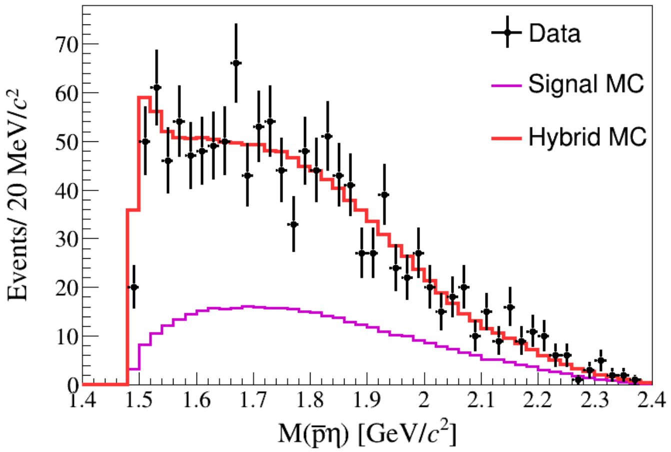


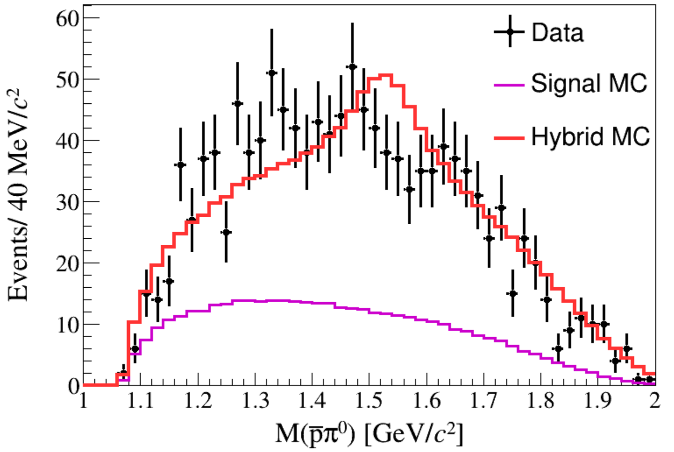


| Decay Chanel | Ratio |
|---|---|
| $\chi_{c2} \to p\bar{p}a_0(980)$ | 8% |
| $\chi_{c2} \to \bar{p}\pi^0 N$ | 14% |
| $\chi_{c2} \to p\eta\bar{N}$ | 16% |
| $\chi_{c2} \to p\pi^0\bar{N}$ | 14% |
| $\chi_{c2} \to \bar{p}\eta N$ | 16% |
| $\chi_{c2} \to p\bar{p}\eta\pi^0$ | 32% |

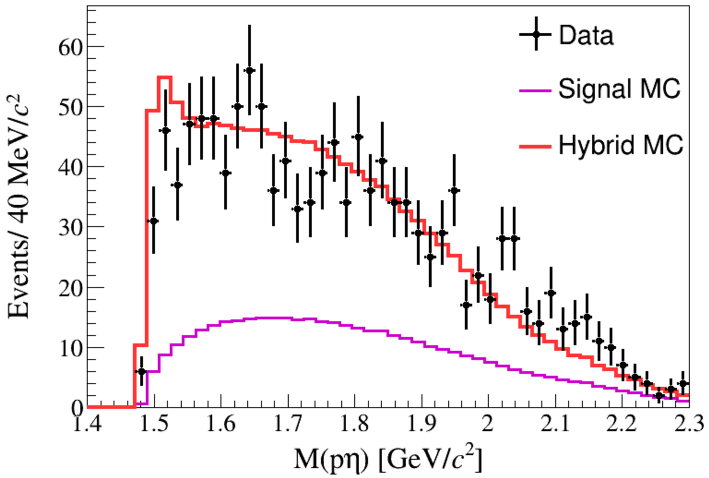


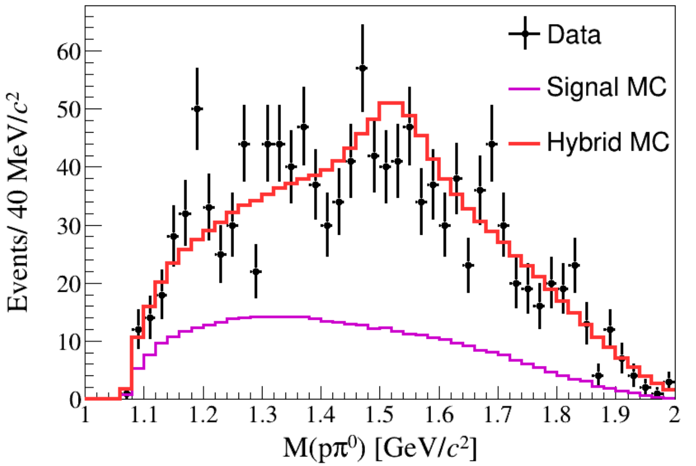

# Analysis I: Intermediate state investigation

| | $\chi_{c0}$ | $\chi_{c1}$ | $\chi_{c2}$ |
|---|---|---|---|
| $\bar{N} \to \bar{p}\pi^0, N \to p\eta$ | 0% | 0% | 0% |
| $\chi_{cJ} \to p\bar{p}a_0(980)$ | 10% | 8% | 8% |
| $\chi_{cJ} \to \bar{p}\pi^0 N$ | 17% | 15% | 14% |
| $\chi_{cJ} \to p\eta\bar{N}$ | 17% | 20% | 16% |
| $\chi_{cJ} \to p\bar{p}\eta\pi^0$ | 22% | 22% | 32% |
| $\chi_{cJ} \to p\pi^0\bar{N}$ | 17% | 15% | 14% |
| $\chi_{cJ} \to \bar{p}\eta N$ | 17% | 20% | 16% |

# Analysis II: Study of $\psi(2S) \rightarrow \Lambda(1520)\bar{\Sigma}^0\eta + \mathrm{c.c.}$

# Analysis II: Outline

- Motivation
- Data Samples
- Event selection
- Intermediate state
- Background analysis
- Branching fraction(BF) measurement
- Summary & Next to do

# Analysis II: Motivation

- The baryon spectroscopy is far from perfect, since many states are either undiscovered or not well established. Baryon decays serves as a powerful tool to address physics problems like the internal structure and fundamental symmetries.
- Many processes have been discovered for the decay of charmonium to three-body (BBV/P) , i.e. $\psi(3686) \to \Lambda\bar{\Lambda}\eta, \pi^0, \eta', \phi$[1] ,or $\psi(3686) \to \Sigma^+\bar{\Sigma}\eta, \omega, \phi$.[2][3]
- Search for possible excited baryon states consisting of $\mathrm{BV/P}$
- At this stage, a data sample based on the 2.7 billion events collected by BESIII at $\psi(3686)$ resonance provides an excellent opportunity to explore. These studies have the potential to greatly improve our understanding of strong decays in particular.


[1] M. Ablikim et al.[BESIII Collaboration], Phys. Rev. D. 106, 072006 (2022)
[2] M. Ablikim et al.[BESIII Collaboration], Phys. Rev. D 106, 112011 (2022)
[3] M. Ablikim et al.[BESIII Collaboration], Phys. Rev. D 106, 112007 (2022)

# Analysis II: Data Samples

| Data set | Number of events | BOSS version |
|---|---|---|
| 09+12 ψ(3686) data | $4.48 \times 10^8$ | 709 |
| 2021 ψ(3686) data | ~$22.5\times 10^8$ | |
| 09+12 ψ(3686) inclusive MC | $5.06\times 10^8$ | |
| 2021 ψ(3686) inclusive MC | ~$23\times 10^8$ | |
| PHSP MC for $\psi(3686) \to pK^-\bar{\Sigma}^0\eta$<br>PHSP MC for $\psi(3686) \to \Lambda(1520)\bar{\Sigma}^0\eta$ | 3 million for each channel (09+12+21) | |
| PHSP MC for $\psi(3686) \to pK^-\bar{\Sigma}^0\pi^0$<br>PHSP MC for $\psi(3686) \to \Lambda(1520)\bar{\Sigma}^0\pi^0$<br>PHSP MC for $\psi(3686) \to \Lambda(1670)\bar{\Sigma}^0\pi^0$ | 3 million for each channel (09+12+21) | |

# Analysis II: Event selection criteria (i) $\psi(3686) \to pK^-\bar{\Sigma}^0\eta, \bar{\Sigma}^0 \to \gamma\bar{\Lambda}, \bar{\Lambda} \to \bar{p}\pi^+, \eta \to \gamma\gamma$

**The charged tracks**

- $|cos\theta| < 0.93$
  - No vertex constraint (the charged tracks originating from $\bar{\Lambda}$ decay)
  - $|V_z| < 10cm, |V_{xy}| < 1cm$ (the charged tracks not originating from $\bar{\Lambda}$ decay)
- $N_{tot} \geq 4$

**PID**

- The tracks are assigned to the particle type with the highest confidence level.
- $N_{\pi^+} \geq 1, N_{\bar{p}} \geq 1, N_p \geq 1, N_{K^-} \geq 1$

**$\bar{\Lambda}$reconstruction**

- 2nd vertex fit

**Vertex Fit**

- The $pK^-$ pair is fitted to a common vertex.

**Good photons**

- $0 \leq TDC \leq 14.$
- Barrel : E > 0.025GeV, $|cos\theta|$ <0.8
- End cap : E > 0.050GeV, 0.86< $|cos\theta|$ <0.92
- $N_\gamma \geq 3$

**Kinematic Fit**

- A four-momentum conservation constraint (4C) kinematic fit under hypothesis of $\psi(3686) \to pK^-\bar{\Lambda}\gamma\gamma\gamma$ is performed.

# Analysis II: Event selection criteria (ii) $\psi(3686) \to pK^-\bar{\Sigma}^0\eta$

Signal MC study: The distinction of the two photons in the $\psi(2S) \to pK^-\bar{\Sigma}^0\eta, \bar{\Sigma}^0 \to \gamma\bar{\Lambda}, \eta \to \gamma\gamma, \bar{\Lambda} \to \bar{p}\pi^+$ process.

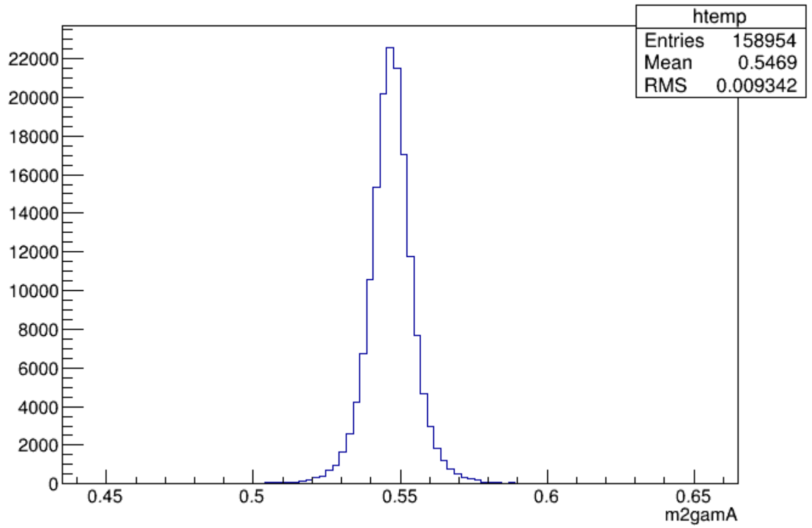


$\eta \to \gamma_{E1\_\mathrm{max}}\ \gamma_{E2\_max}$

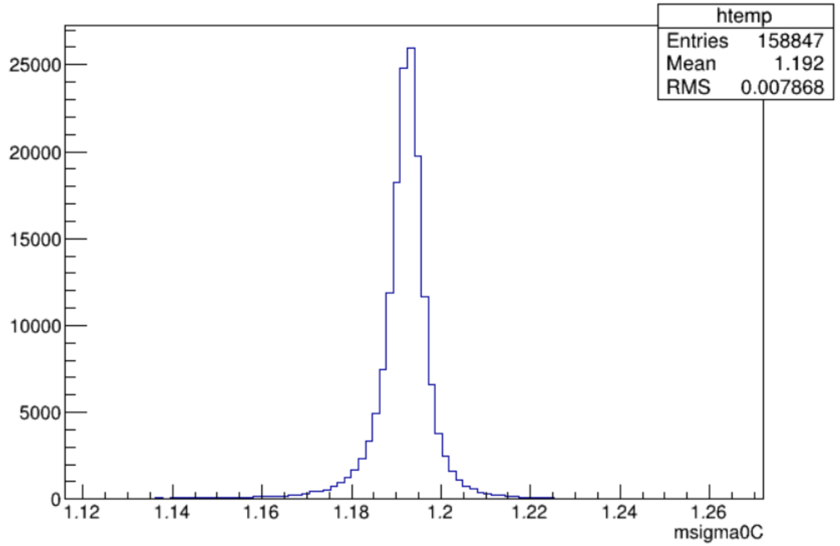


$\bar{\Sigma}^0 \to \gamma_{E3\_max}\bar{\Lambda}$

# Analysis II: Event selection criteria (iii) $\psi(3686) \to pK^-\bar{\Sigma}^0\eta$

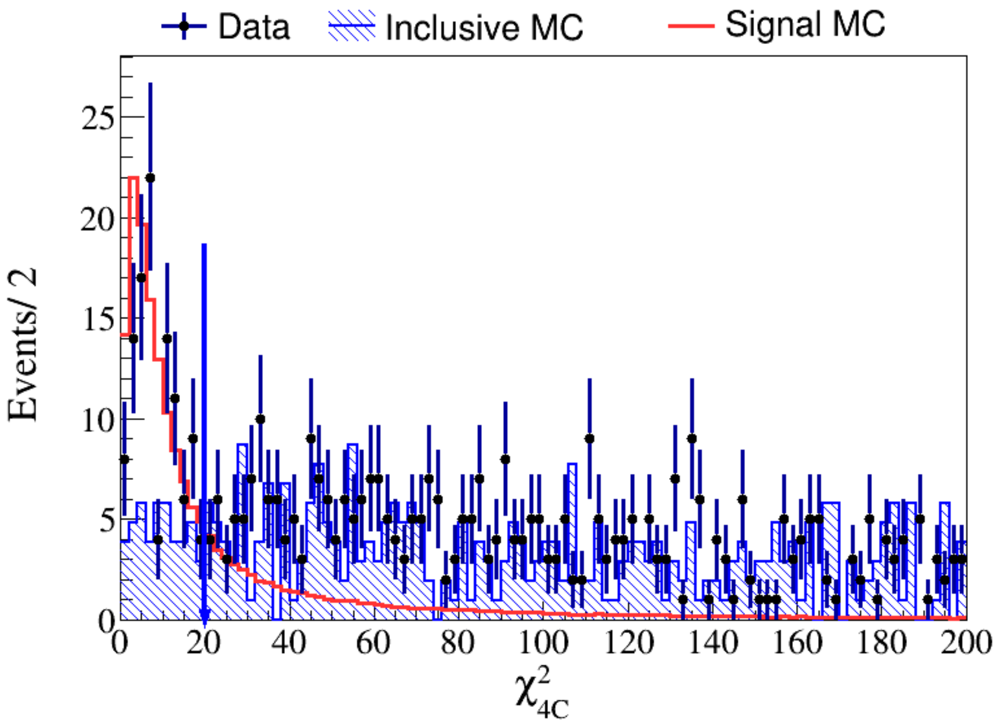


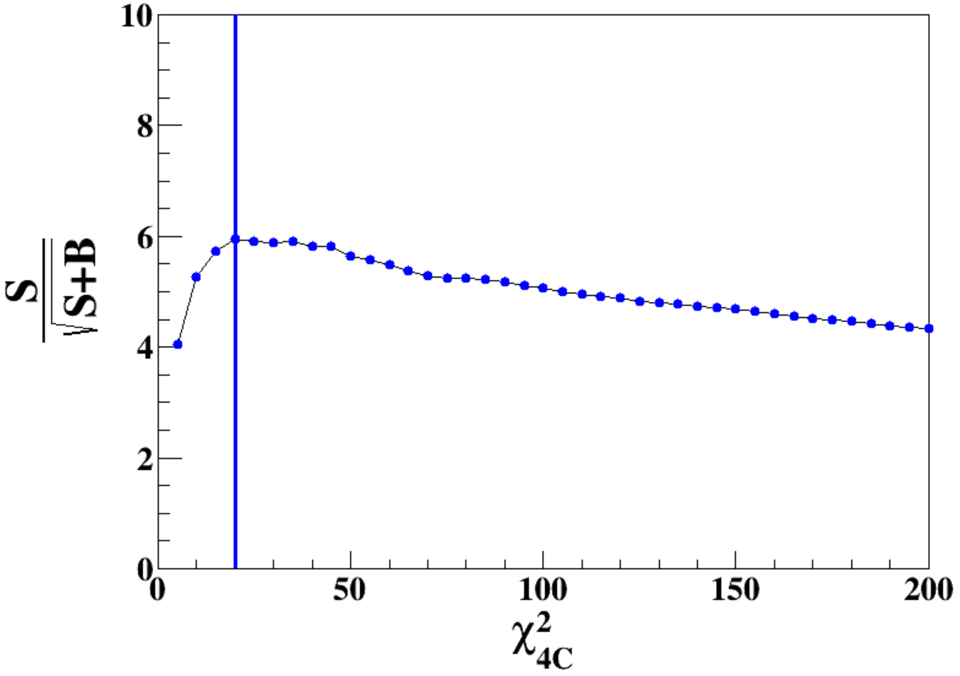


$$\chi^2_{4C} < 20$$

# Analysis II: Event selection criteria (iv) $\psi(3686) \to pK^-\bar{\Sigma}^0\eta$

- The $J/\psi$-related backgrounds like $\psi(2S) \to \eta J/\psi$ is vetoed by the requirements on the $\gamma_1\gamma_2$ recoil mass windows

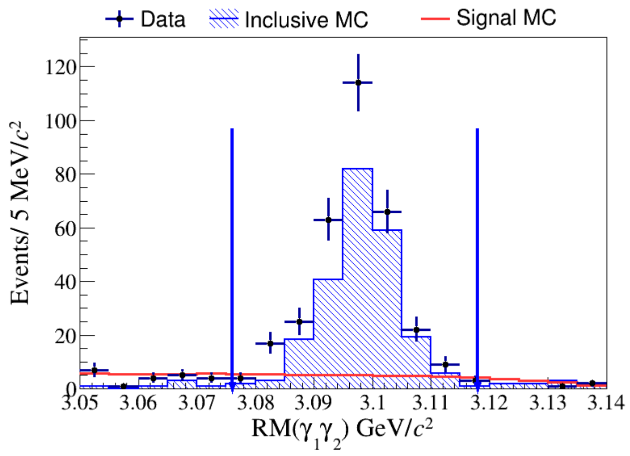


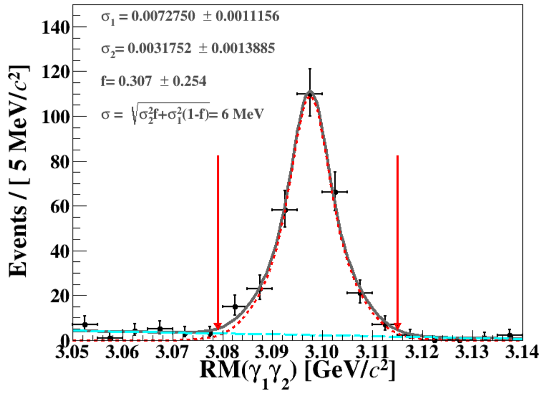


$$|RM(\gamma_1\gamma_2) - m_{J/\psi}| > 18MeV/c^2$$

- The wrong photons backgrounds like $\psi(2S) \to \pi^0\gamma_2\bar{\Lambda}pK^-$ is vetoed by the requirements on the $\gamma_1\gamma_3$ recoil mass windows

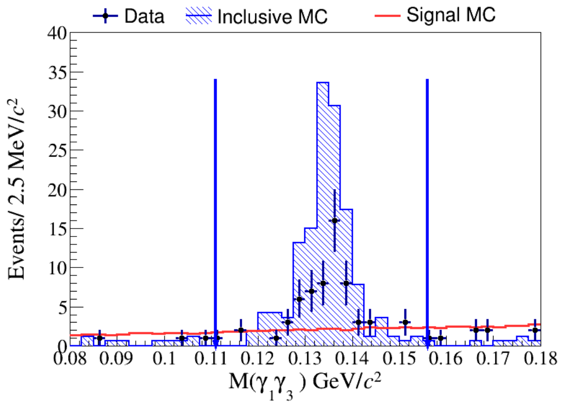


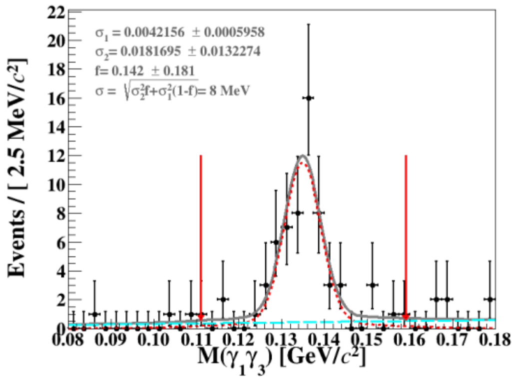


$$|M(\gamma_1\gamma_3) - m_{\pi^0}| > 24MeV/c^2$$

# The distribution of the 2D scatter plot of $M(\gamma_1\gamma_2) v.s. M(\overline{\Sigma}^0)$

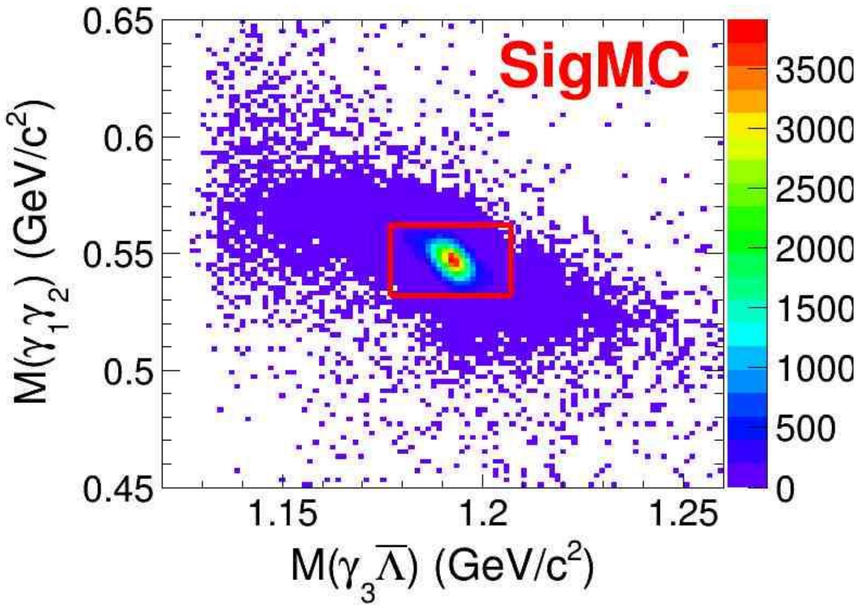


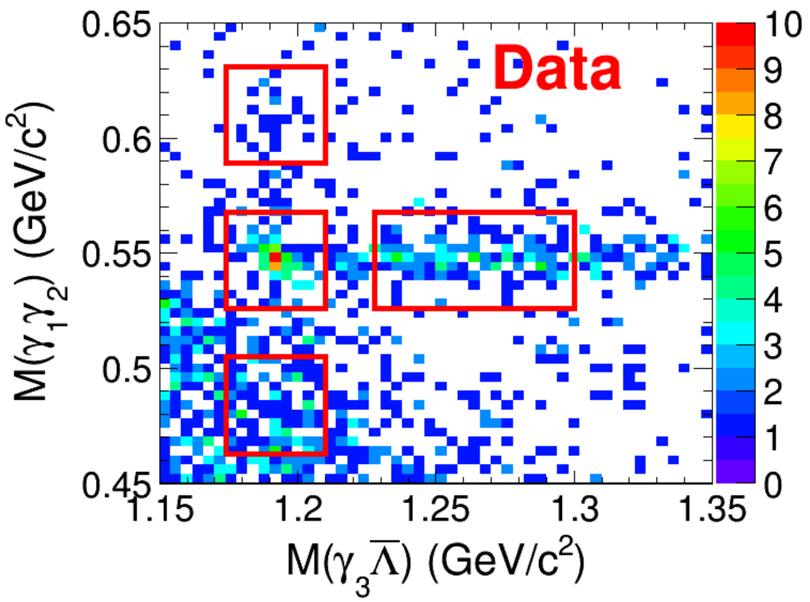


MC: $\psi(2S) \to pK^-\overline{\Sigma}^0\eta, \overline{\Sigma}^0 \to \gamma\overline{\Lambda}, \eta \to \gamma\gamma, \overline{\Lambda} \to \overline{p}\pi^+$

# Analysis II: Intermediate state $\psi(3686) \to pK^-\bar{\Sigma}^0\eta$

$\psi(2S) \to \Lambda(1520)\bar{\Sigma}^0\eta$

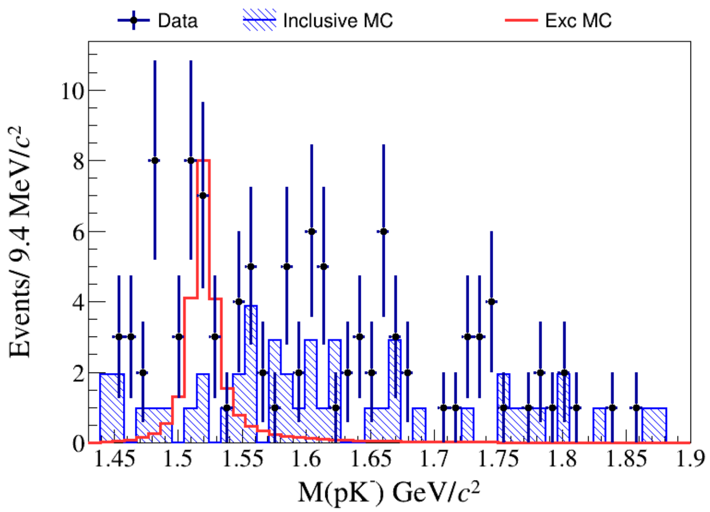


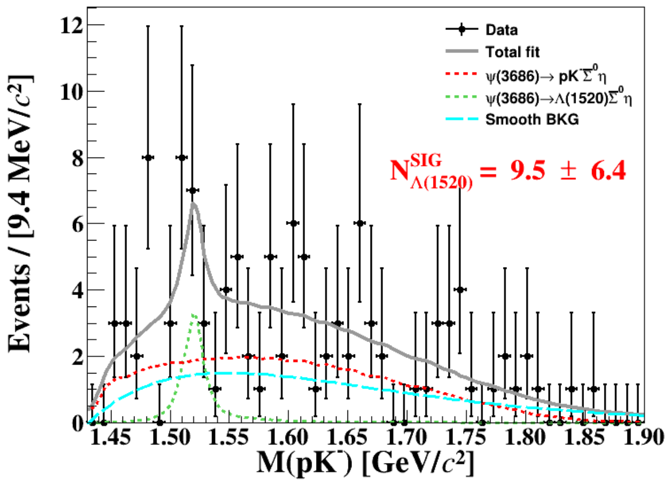


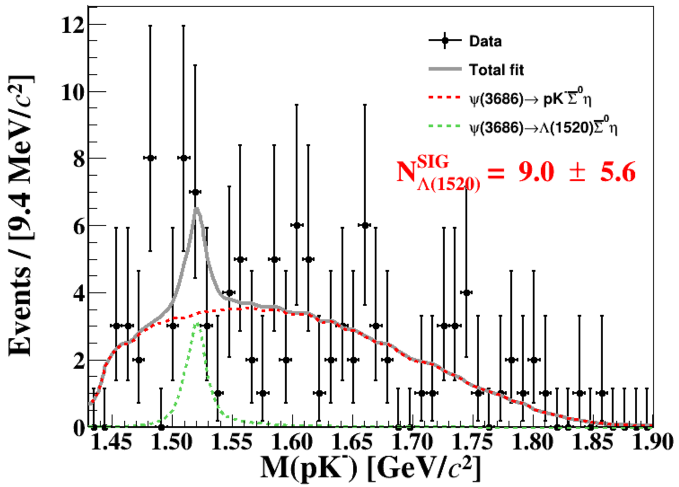


**Possible intermediate state structures were observed in the invariant mass spectra of $pK^-$**

# Analysis II: Branching fraction measurement $\psi(3686) \to pK^-\bar{\Sigma}^0\eta$

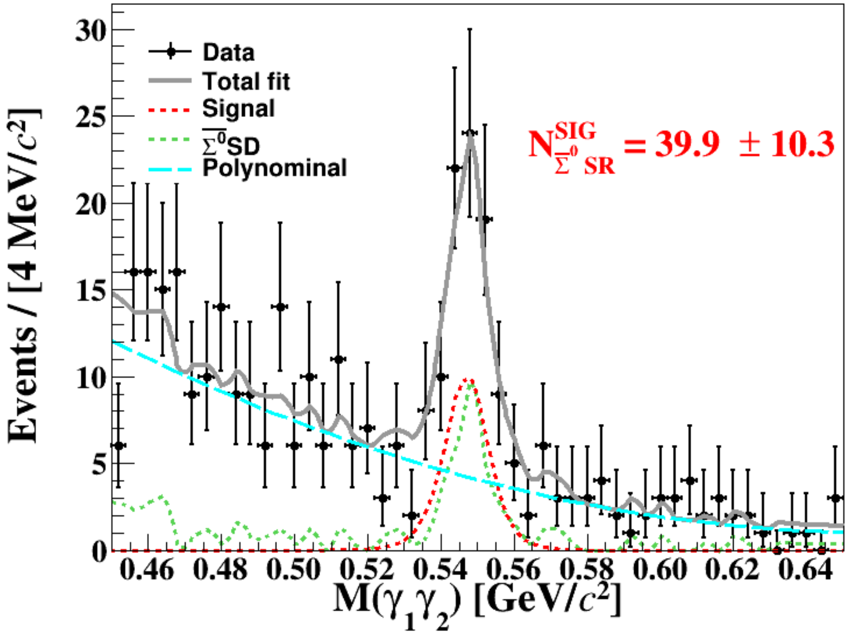


- Fit method: Sig.MC+ $2^{nd}$-order Polynomial
- $Br(\psi(3686) \to pK^-\bar{\Sigma}^0\eta) = \frac{N^{obs}}{N^{data}_{\psi(3686)} \cdot B(\bar{\Sigma}^0 \to \gamma\bar{\Lambda}) \cdot B(\eta \to \gamma\gamma) \cdot B(\bar{\Lambda} \to \bar{p}\pi^+) \cdot \varepsilon}$
- $N^{data}_{\psi(3686)} = (2.26 + 0.448) Billion$
- $Br(\bar{\Sigma}^0 \to \gamma\bar{\Lambda}) = 1$
- $Br(\bar{\Lambda} \to \bar{p}\pi^+) = 64.1\%$
- $Br(\eta \to \gamma\gamma) = 39.36\%$
- $\varepsilon = 4.55\%$
- BF($\boldsymbol{\psi(3686) \to pK^-\bar{\Sigma}^0\eta}$ )~$1 \times 10^{-6}$
- It is the same level as the branching fraction of $\boldsymbol{\psi(3686) \to pK^-\bar{\Lambda}\eta}$ [1]

| Mode | $N^{obs}$ | ε(%) | BR | Significance(σ) |
|---|---|---|---|---|
| $\psi(3686) \to pK^-\bar{\Sigma}^0\eta$ | 39.9 | 5.31 | ~$10^{-6}$ | ~4.4 |

[1] Lin ZHU et al, Search for $\psi(3686) \to \Lambda(1520)\bar{\Lambda}\eta/\Lambda(1670)\bar{\Lambda}\eta$+c.c.,[Online] Nov.$15^{th}$,2023 for Charmonium Group Meeting.

# Analysis II: Event selection criteria (i) $\psi(3686) \to pK^-\bar{\Sigma}^0\pi^0, \bar{\Sigma}^0 \to \gamma\bar{\Lambda}, \bar{\Lambda} \to \bar{p}\pi^+$

**The charged tracks**

- $|cos\theta| < 0.93$
  - No vertex constraint (the charged tracks originating from $\bar{\Lambda}$ decay)
  - $|V_z| < 10cm, |V_{xy}| < 1cm$ (the charged tracks not originating from $\bar{\Lambda}$ decay)
- $N_{tot} \geq 4$

**PID**

- The tracks are assigned to the particle type with the highest confidence level.
- $N_{\pi^+} \geq 1, N_{\bar{p}} \geq 1, N_p \geq 1, N_{K^-} \geq 1$

**$\bar{\Lambda}$ reconstruction**

- 2nd vertex fit

**$\pi^0$ and $\bar{\Sigma}^0$reconstruction**

- $\Delta_{\min} = \sqrt{(M_{\bar{\Sigma}^0} - m_{\bar{\Sigma}^0})^2 + (M_{\pi^0} - m_{\pi^0})^2} \Rightarrow \bar{\Sigma}^0_{min},\ \pi^0_{min}$

**Vertex Fit**

- The $pK^-$ pair is fitted to a common vertex.

**Good photons**

- $0 \leq TDC \leq 14.$
- Barrel : E > 0.025GeV, $|cos\theta|$ <0.8
- End cap : E > 0.050GeV, 0.86< $|cos\theta|$ <0.92
- $N_\gamma \geq 3$

**Kinematic Fit**

- A four-momentum conservation constraint (4C) kinematic fit under hypothesis of $\psi(3686) \to pK^-\bar{\Lambda}\gamma\gamma\gamma$ is performed.

# Analysis II: Event selection criteria (ii) $\psi(3686) \to pK^-\bar{\Sigma}^0\pi^0, \bar{\Sigma}^0 \to \gamma\bar{\Lambda}, \bar{\Lambda} \to \bar{p}\pi^+$

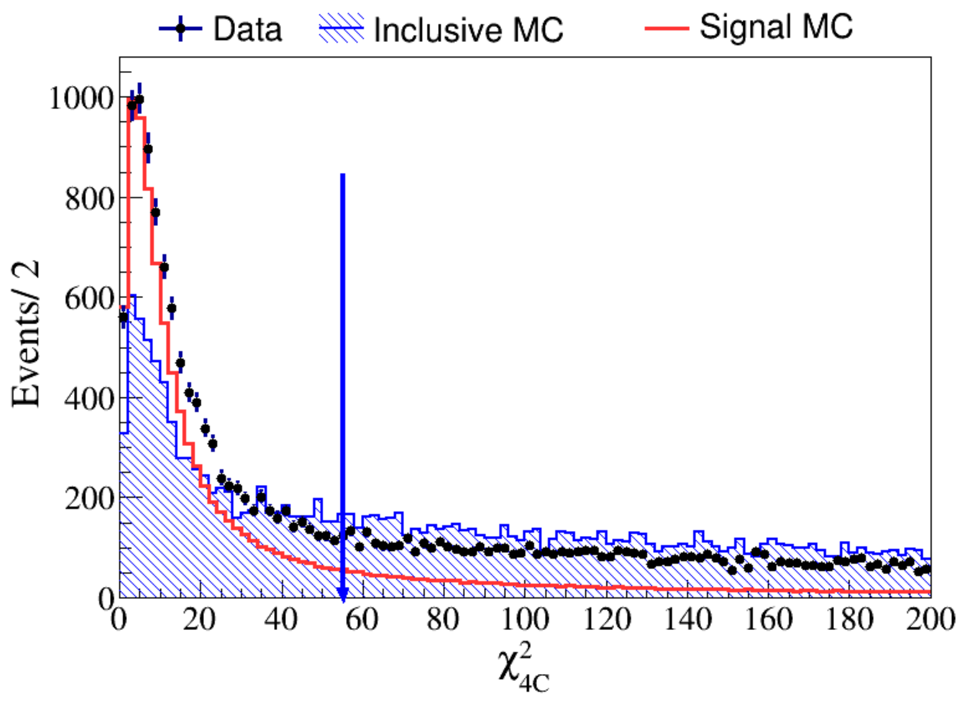


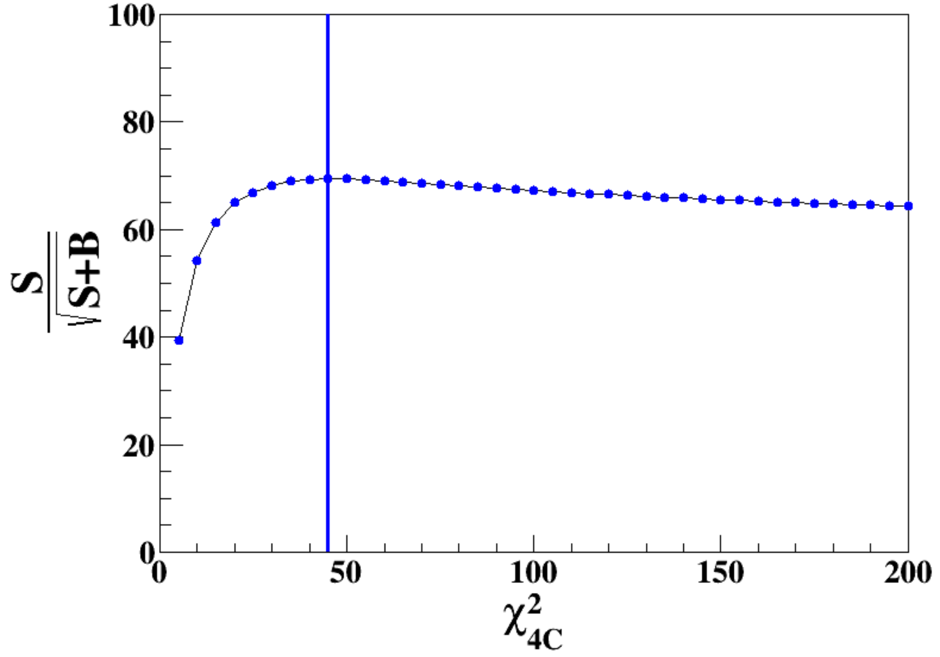


$$\chi^2_{4C} < 45$$

# Analysis II: Event selection criteria (iii) $\psi(3686) \rightarrow pK^{-}\bar{\Sigma}^{0}\pi^{0}, \bar{\Sigma}^{0} \rightarrow \gamma\bar{\Lambda}, \bar{\Lambda} \rightarrow \bar{p}\pi^{+}$

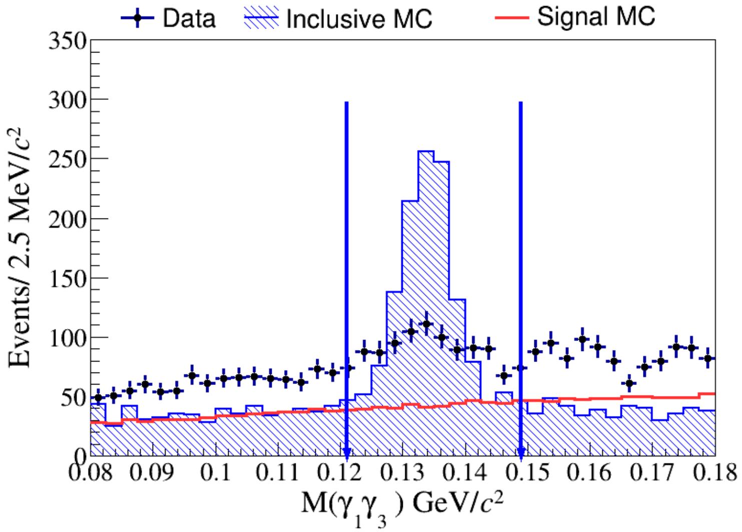


**Negligible**

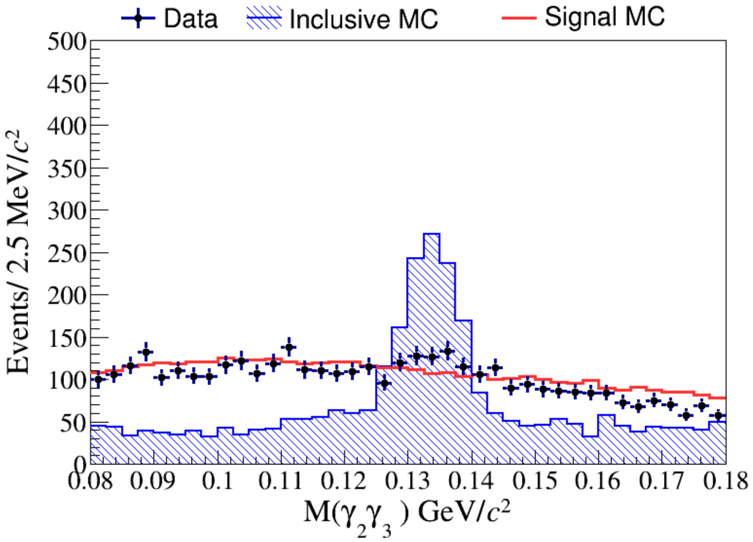


**Negligible**

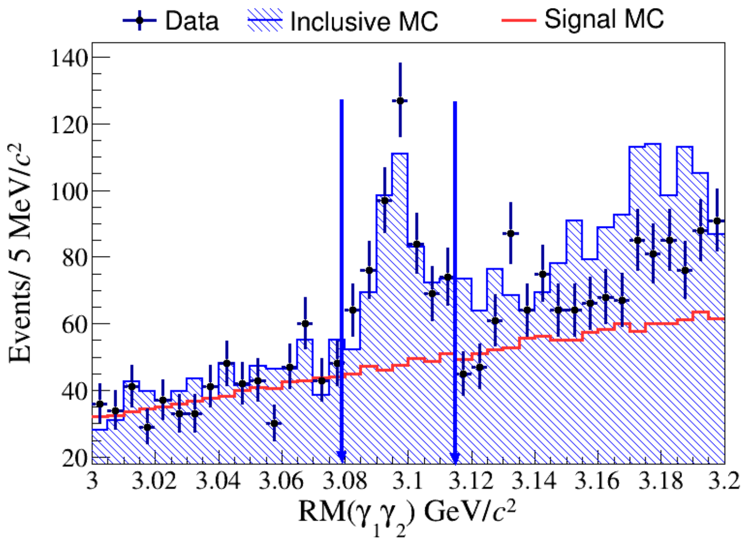


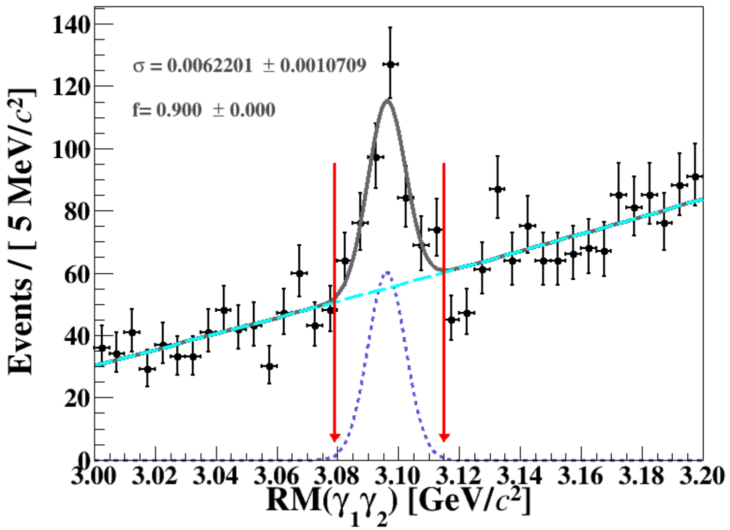


$|RM(\gamma_1\gamma_2) - m_{J/\psi}| > 18MeV/c^2$

# Analysis II: Event selection criteria (iv) $\psi(3686) \to pK^-\bar{\Sigma}^0\pi^0, \bar{\Sigma}^0 \to \gamma\bar{\Lambda}, \bar{\Lambda} \to \bar{p}\pi^+$

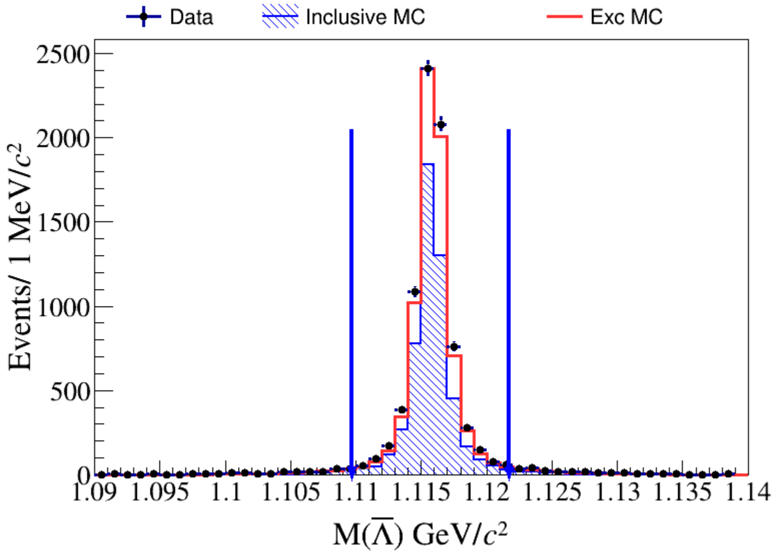


$|M(\bar{\Lambda}) - 1.157| < 6MeV/c^2$

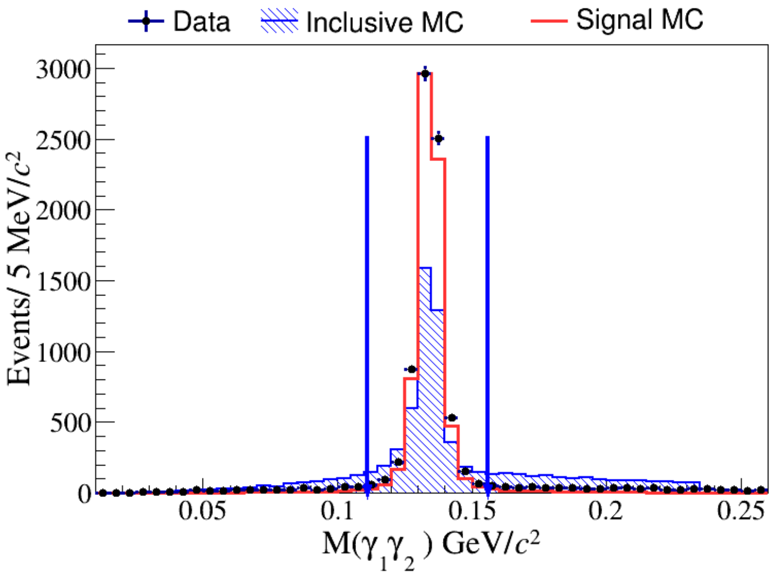


$|M(\pi^0) - 0.135| < 24MeV/c^2$

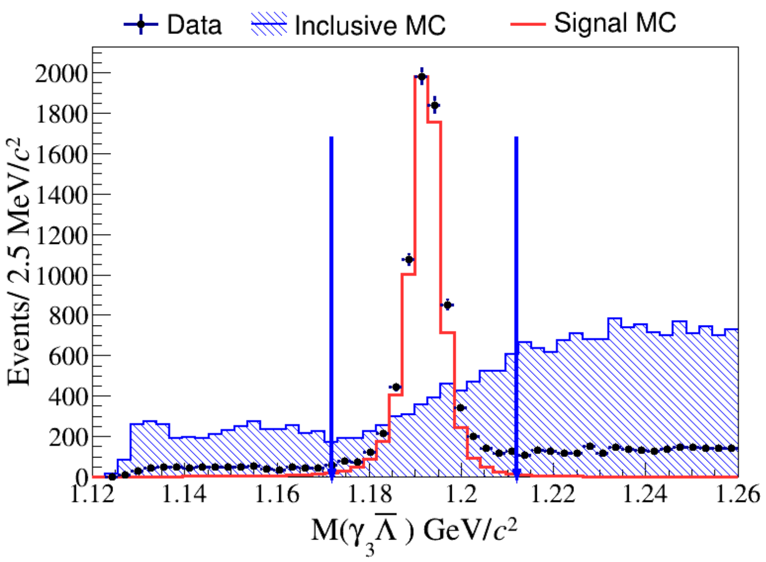


$|M(\bar{\Sigma}^0) - 1.192| < 18MeV/c^2$

# The distribution of the 2D scatter plot of $M(\gamma_1\gamma_2) v.s. M(\bar{\Sigma}^0)$

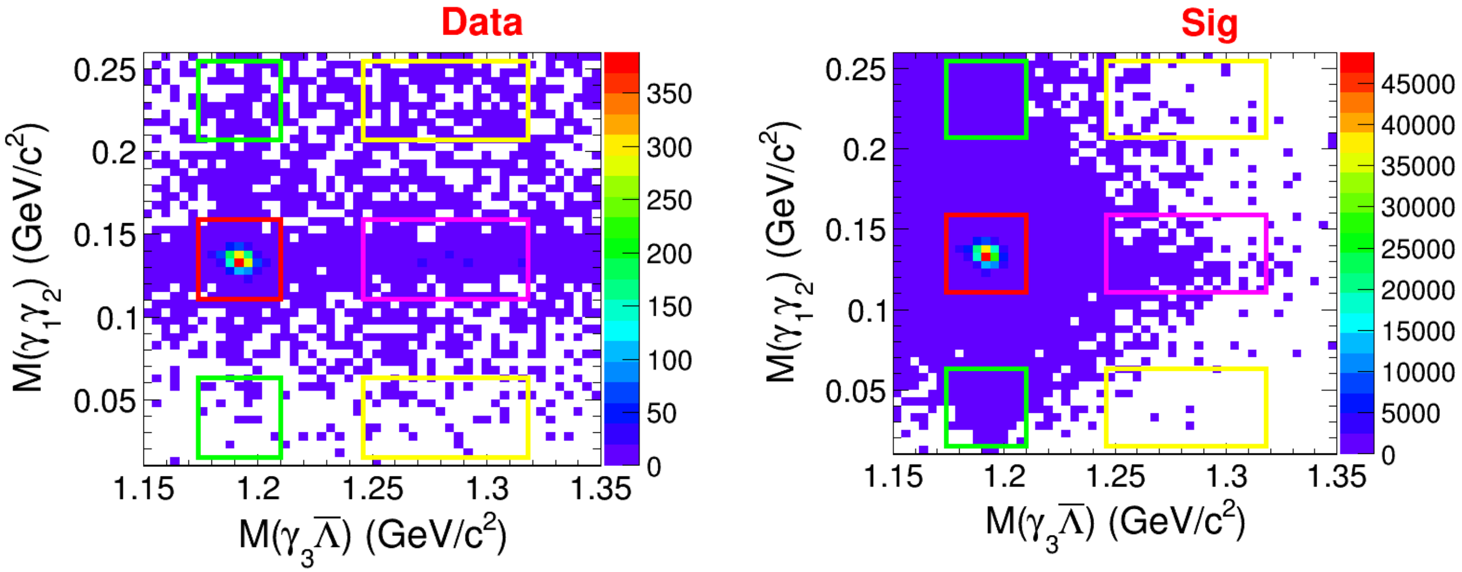


MC: $\psi(2S) \to pK^-\bar{\Sigma}^0\pi^0, \bar{\Sigma}^0 \to \gamma\bar{\Lambda}, \pi^0 \to \gamma\gamma, \bar{\Lambda} \to \bar{p}\pi^+$

# Analysis II: Intermediate state $\psi(3686) \rightarrow pK^-\bar{\Sigma}^0\pi^0$

$\psi(2S) \rightarrow \Lambda(1520)\bar{\Sigma}^0\pi^0$

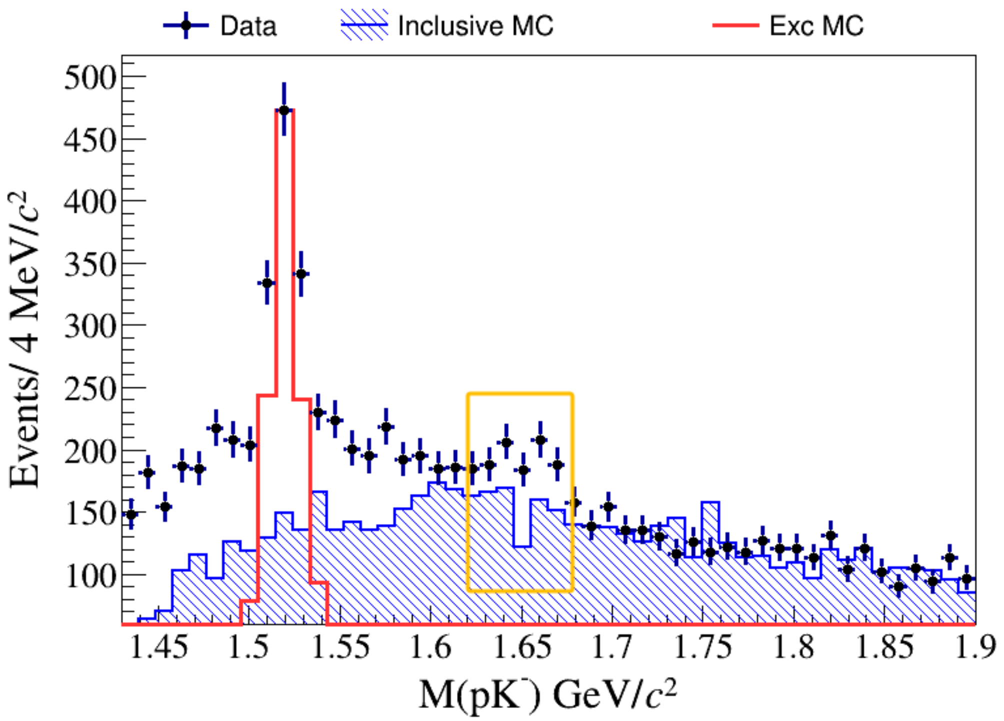


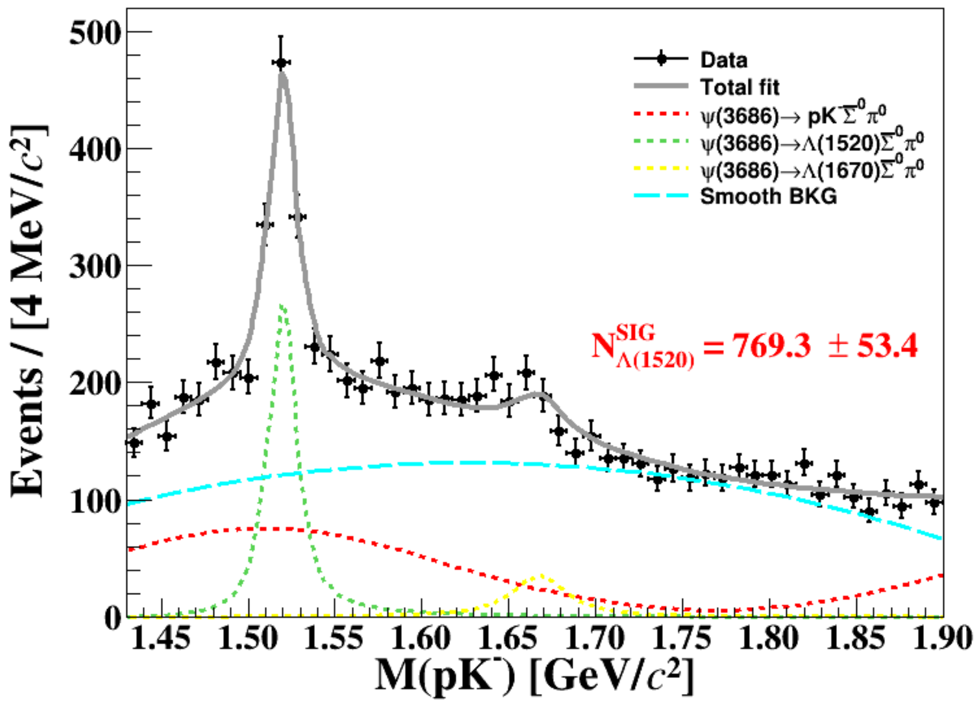


**Intermediate state structures were observed in the invariant mass spectra of** $pK^-$

# Analysis II: Branching fraction measurement $\psi(3686) \to pK^-\bar{\Sigma}^0\pi^0$

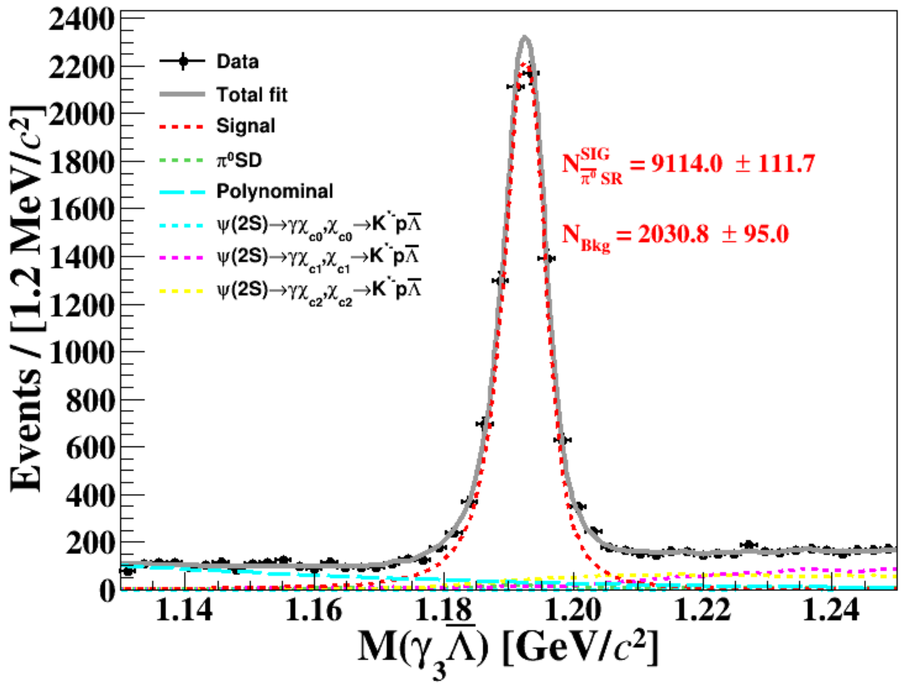


- Fit method: Sig.MC+ 2nd-order Chebychev
- $Br(\psi(3686) \to pK^-\bar{\Sigma}^0\pi^0) = \frac{N^{obs}}{N^{data}_{\psi(3686)} \cdot B(\bar{\Sigma}^0 \to \gamma\bar{\Lambda}) \cdot B(\pi^0 \to \gamma\gamma) \cdot B(\bar{\Lambda} \to \bar{p}\pi^+) \cdot \varepsilon}$
- $N^{data}_{\psi(3686)} = (2.26 + 0.448) Billion$
- $Br(\bar{\Sigma}^0 \to \gamma\bar{\Lambda}) = 1$
- $Br(\bar{\Lambda} \to \bar{p}\pi^+) = 64.1\%$
- $Br(\pi^0 \to \gamma\gamma) = 98.82\%$
- $\varepsilon = 10.56\%$

| Mode | $N^{obs}$ | ε(%) | BR |
|---|---|---|---|
| $\psi(3686) \to pK^-\bar{\Sigma}^0\pi^0$ | 9114.0±117 | 10.56 | $\sim 1 \times 10^{-5}$ |

# ➢Summary & Next to do

## ➢ Summary

Using about 2.7 billion $\psi(3686)$ data sample collected at BESIII in 2009, 2012 ,and 2021:

- ✓ All selection criteria have been optimized for $\psi(3686) \to pK^-\bar{\Sigma}^0\eta/\pi^0$, and essentially no peaking background is observed under all selection criteria.
- ✓ The signal of the decay of $\psi(3686) \to pK^-\bar{\Sigma}^0\eta/\pi^0$ was observed for the first time. At the same time, a possible excited state $\Lambda(1520)$ was also observed.

## ➢ Next to do

- ✓ Study of the conjugate channels
- ✓ Further studying the possible peaking backgrounds
- ✓ Further studying the potential intermediate states
- ✓ Further studying the impact of sideband of intermediate states
- ✓ Studying the systematic uncertainties

# Back Up

$$\psi(2S) \to pK^-\bar{\Sigma}^0\eta, \bar{\Sigma}^0 \to \gamma\bar{\Lambda}, \eta \to \gamma\gamma, \bar{\Lambda} \to \bar{p}\pi^+$$

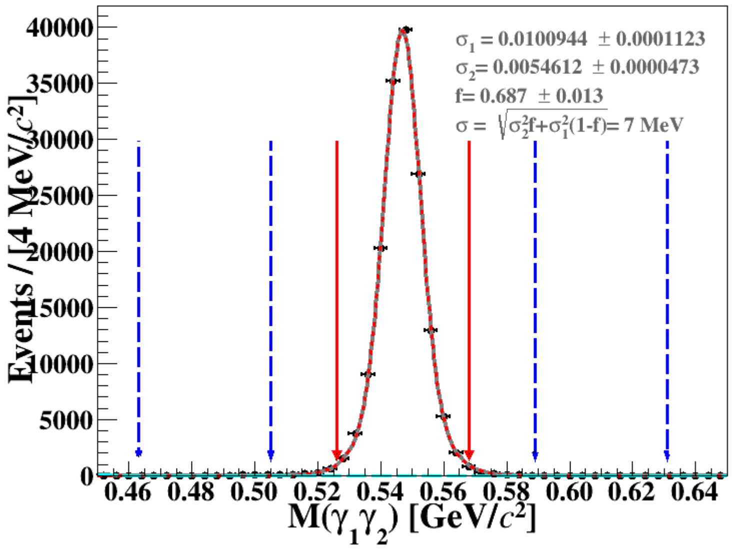


$|M(\gamma_1\gamma_2) - m_\eta| < 21MeV/c^2$

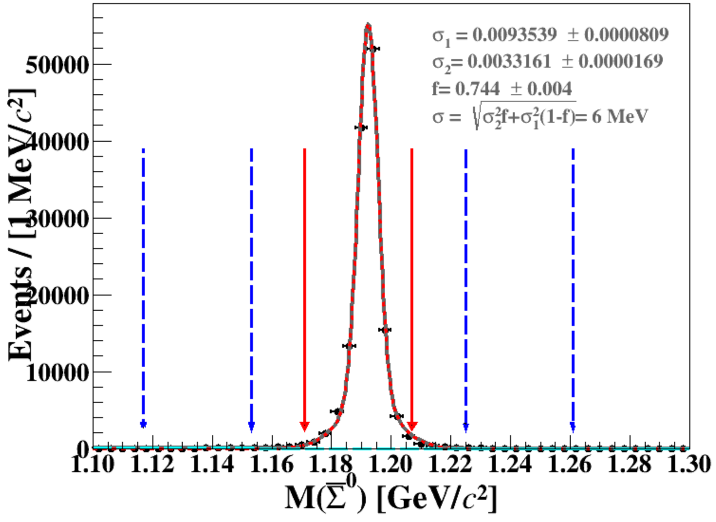


$|M(\bar{\Sigma}^0) - 1.192| < 18MeV/c^2$

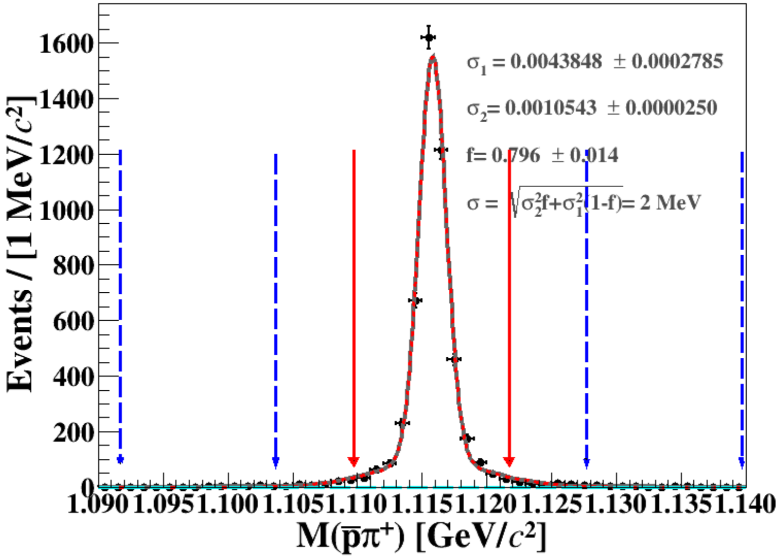


$|M(\bar{\Lambda}) - 1.157| < 6MeV/c^2$

Analysis of $\psi(2S) \to pK^-\bar{\Sigma}^0\pi^0, \bar{\Sigma}^0 \to \gamma\bar{\Lambda}, \pi^0 \to \gamma\gamma, \bar{\Lambda} \to \bar{p}\pi^+$

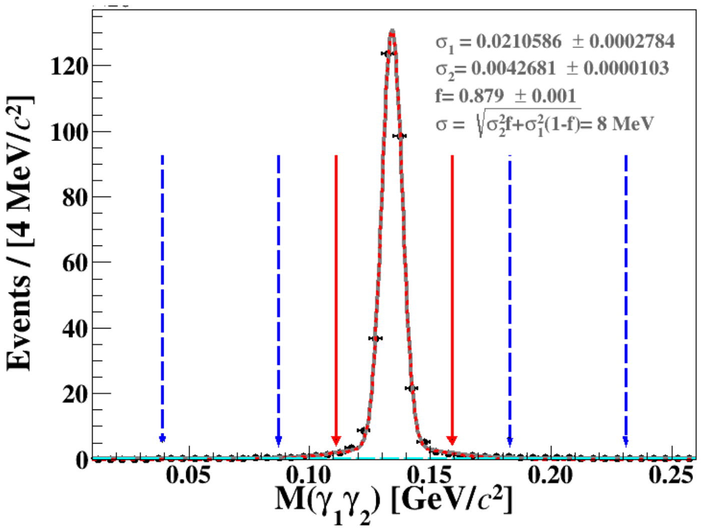


$|M(\gamma_1\gamma_2) - m_{\pi^0}| < 24MeV/c^2$

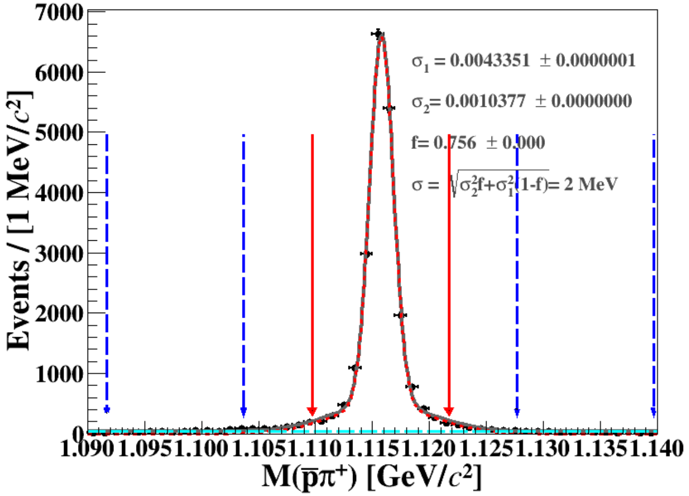


$|M(\bar{\Lambda}) - 1.157| < 6MeV/c^2$

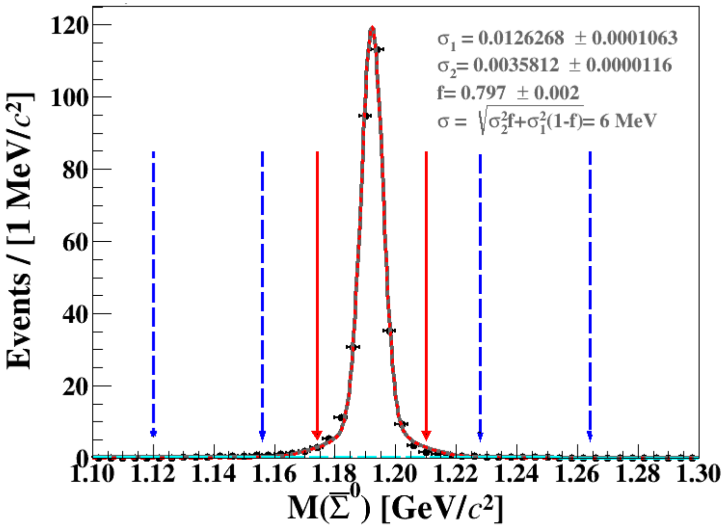


$|M(\bar{\Sigma}^0) - 1.192| < 18MeV/c^2$

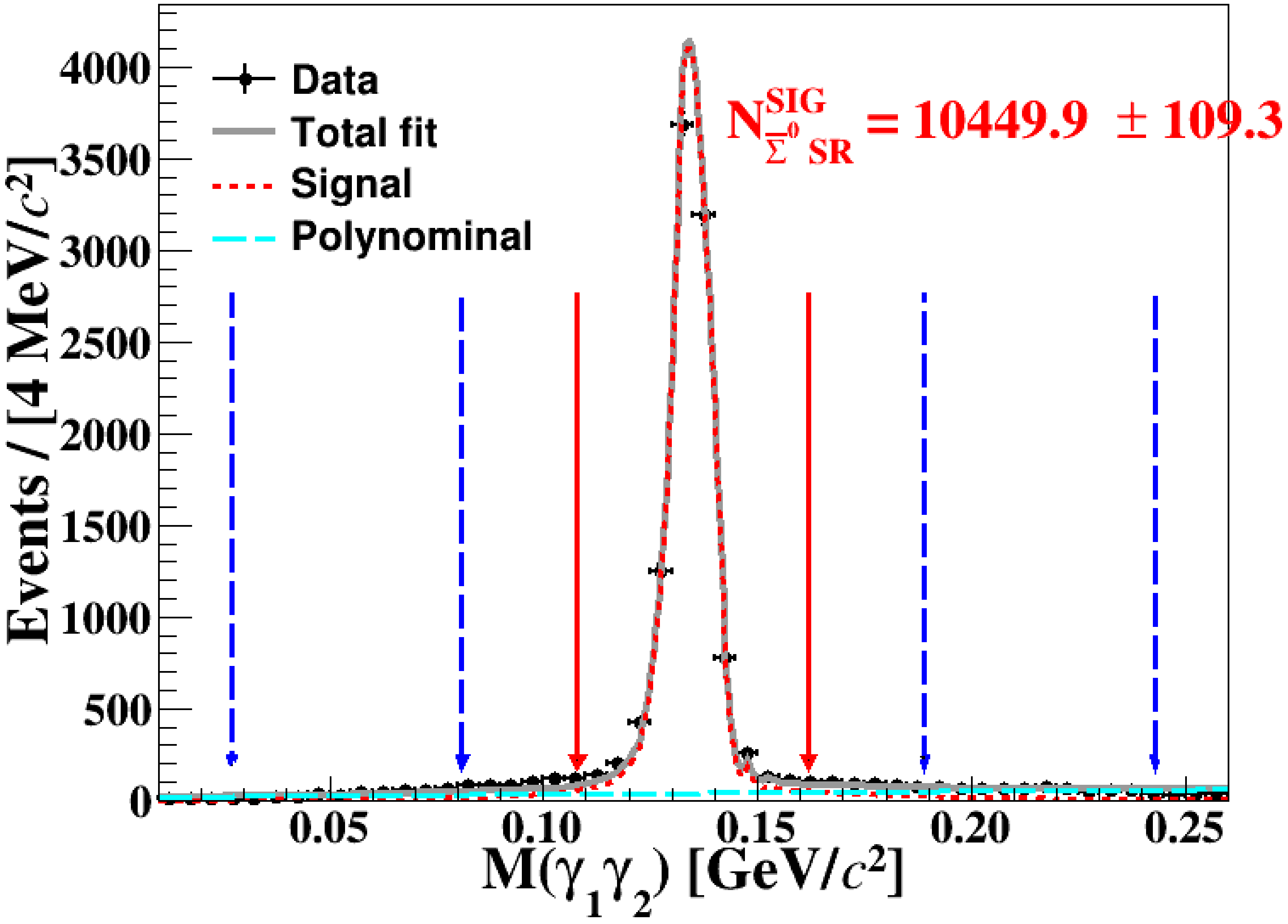


通过pi0SD区估计Sigma0峰状本底事例数大约413.5

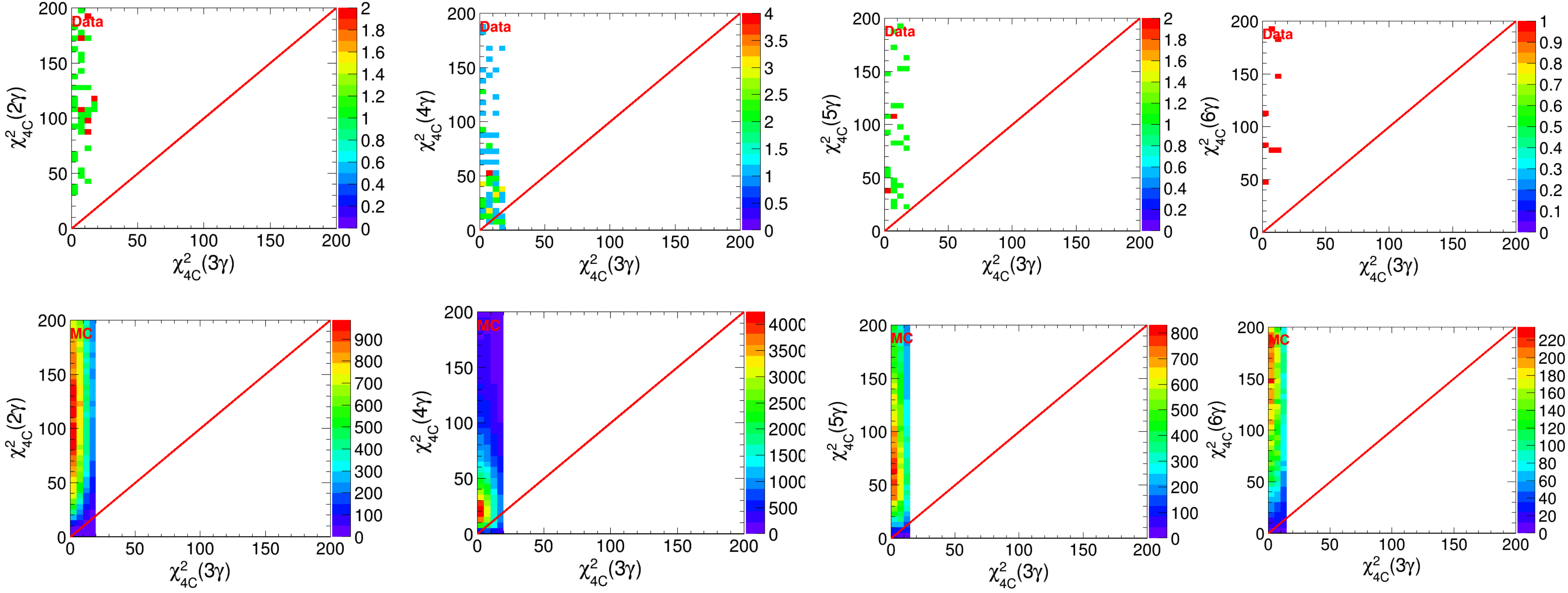


**Due to the small number of events, adding $\chi^2_{4C}(3\gamma) < \chi^2_{4C}(4\gamma)$ did not veto many events, but instead it affected the efficiency.**

$$\psi(2S) \to pK^-\bar{\Sigma}^0\eta, \bar{\Sigma}^0 \to \gamma\bar{\Lambda}, \eta \to \gamma\gamma, \bar{\Lambda} \to \bar{p}\pi^+$$

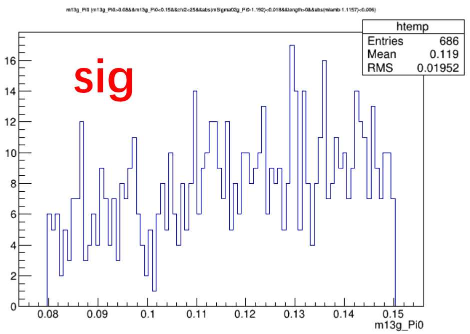


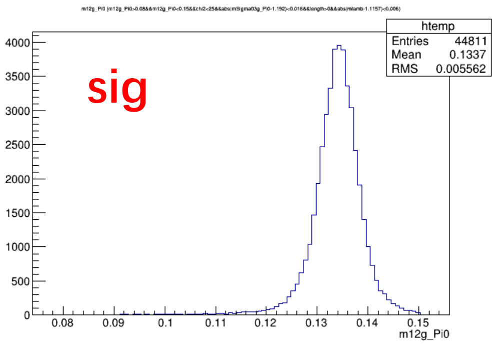


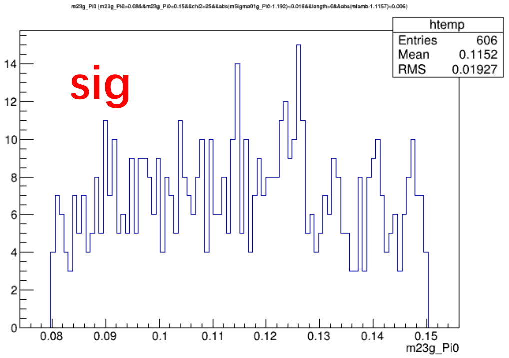


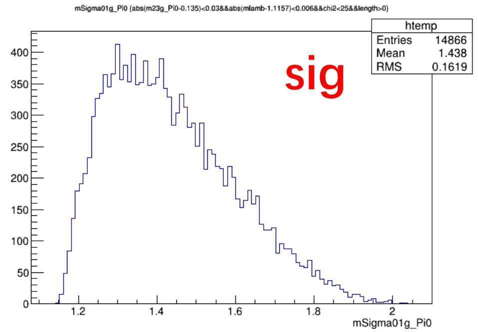


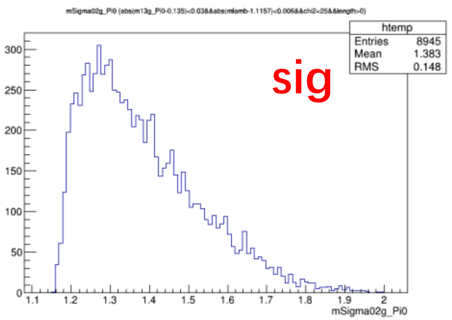


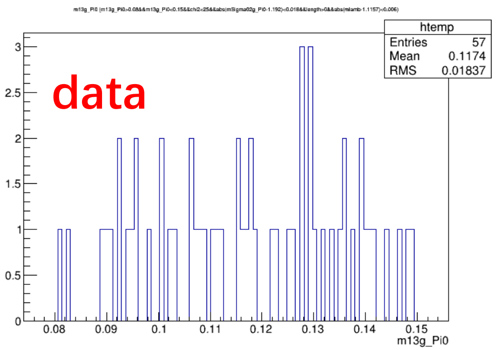


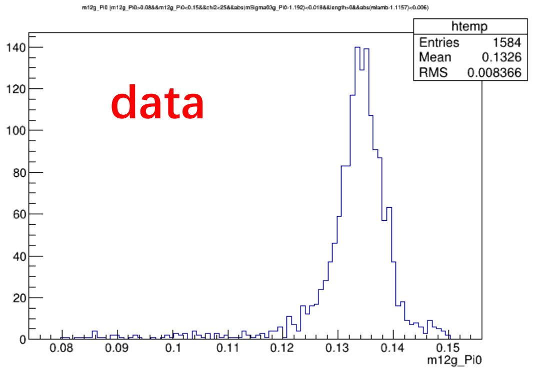


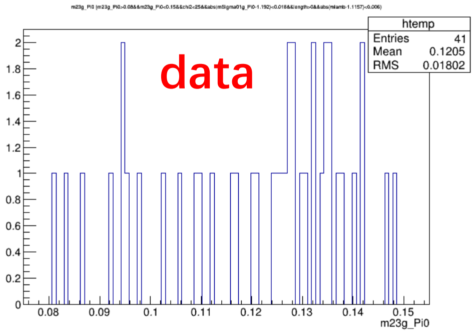


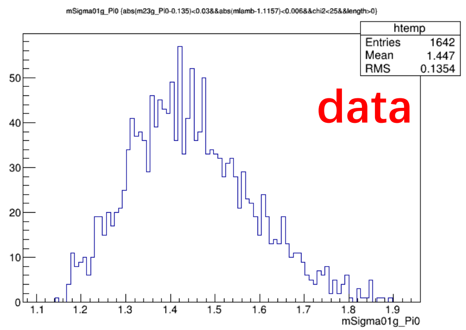


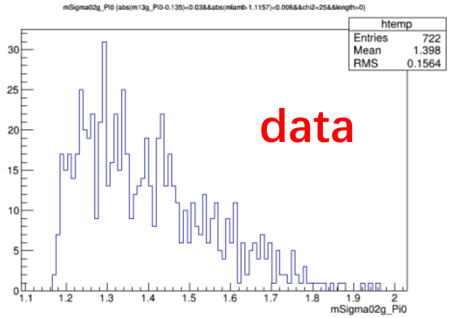


M13g

M12g

M23g

mSigma01g

mSigma02g

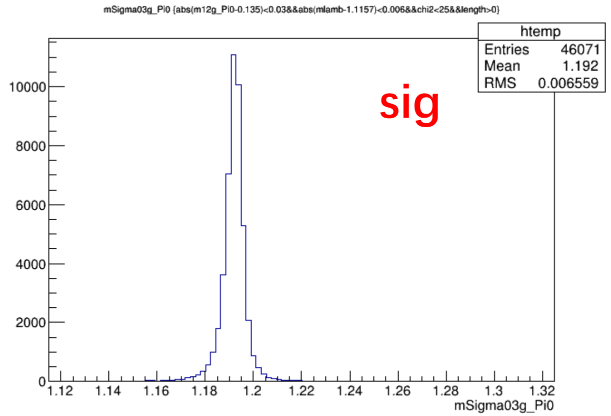


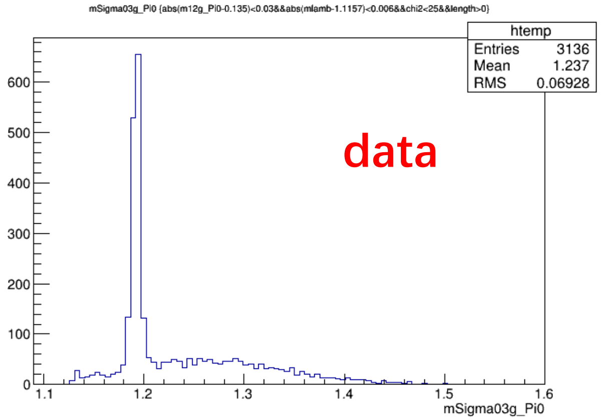


mSigma03g

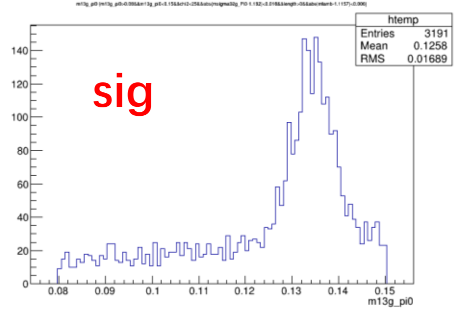


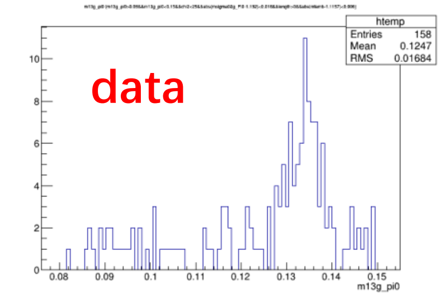


M13g

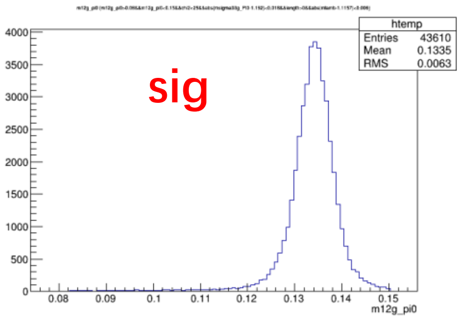


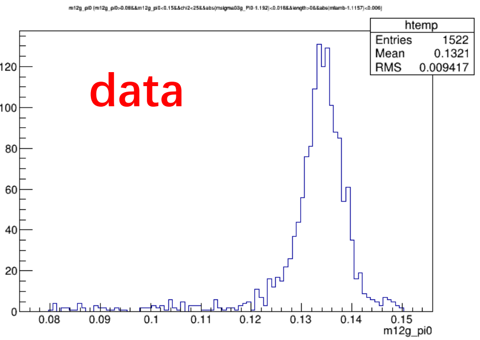


M12g

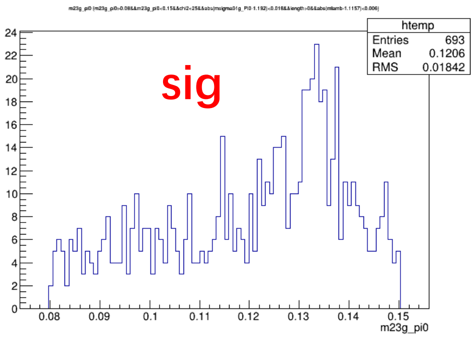


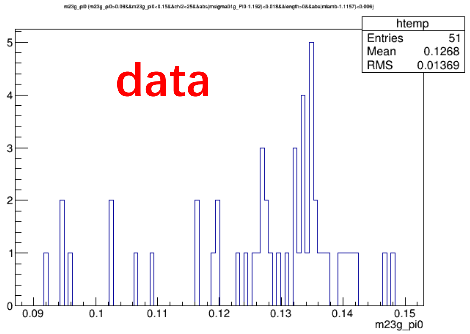


M23g

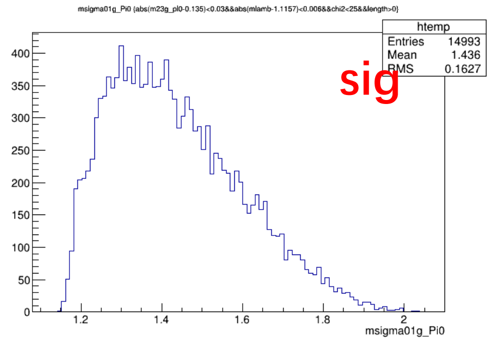


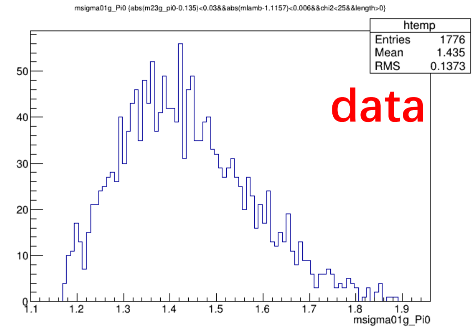


mSigma01g

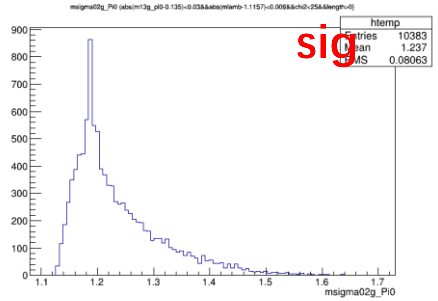


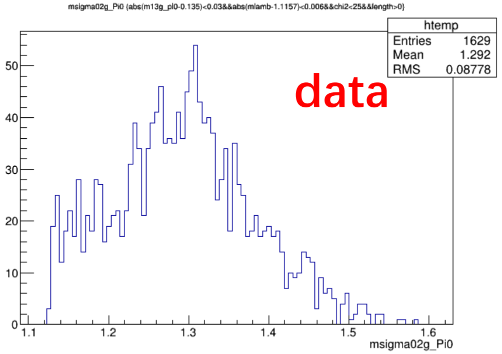


mSigma02g

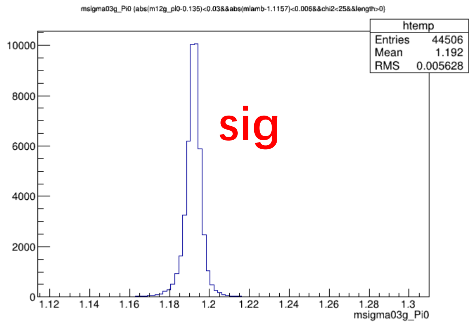


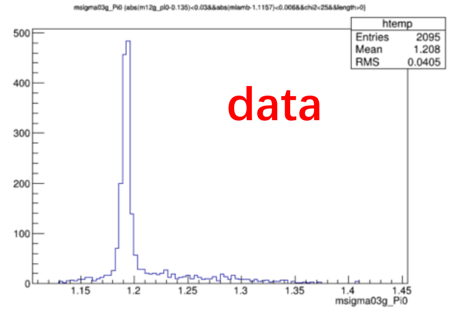


mSigma03g

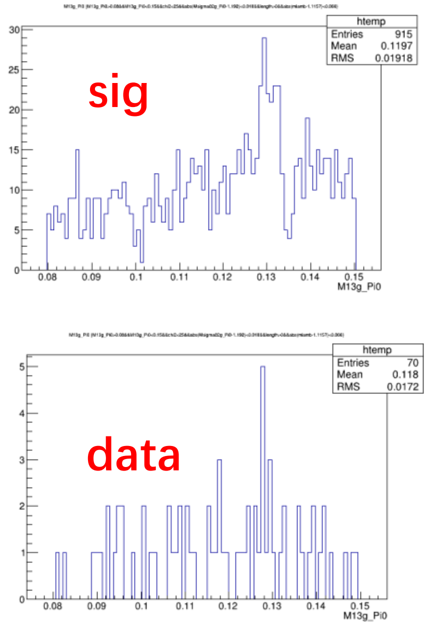


M13g

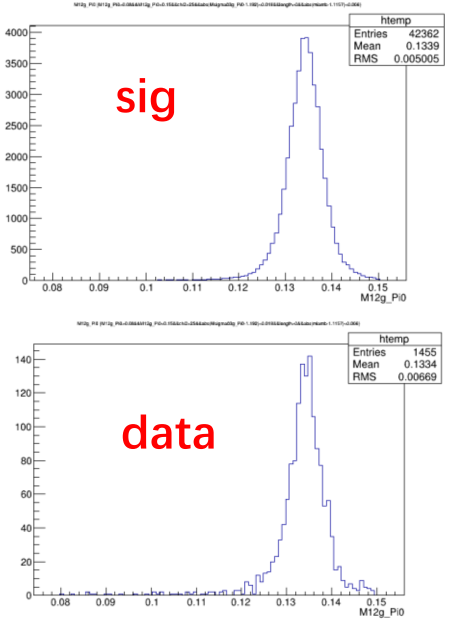


M12g

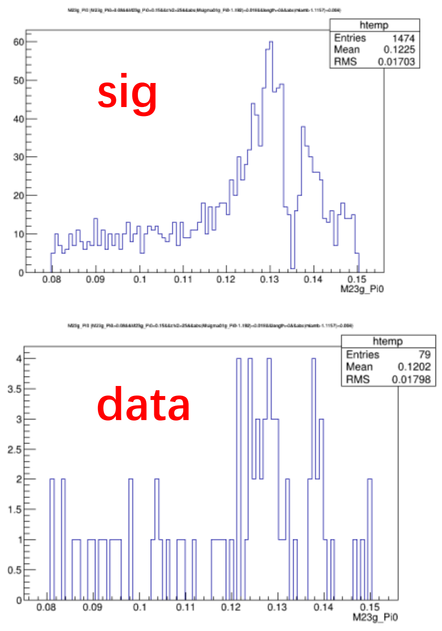


M23g

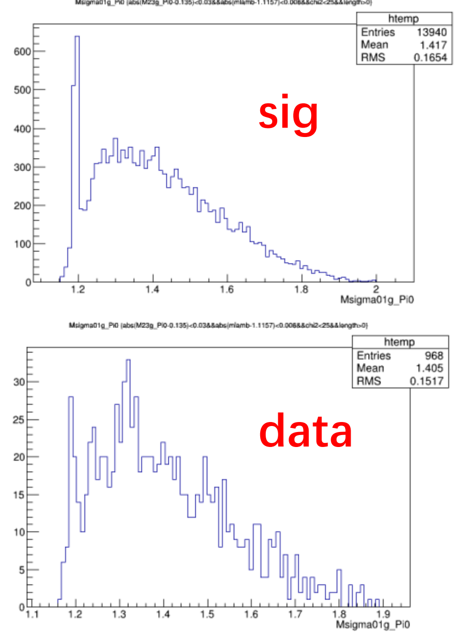


mSigma01g

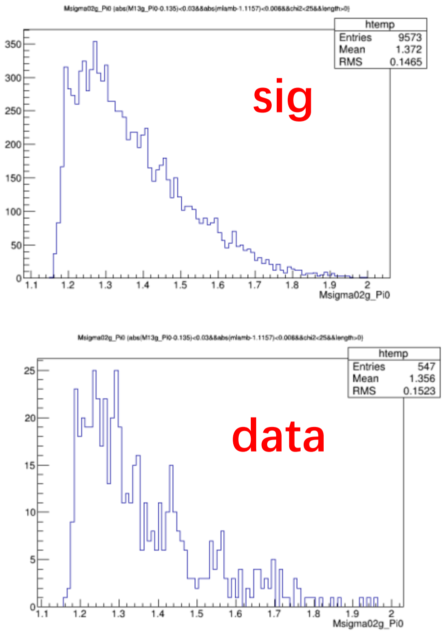


mSigma02g

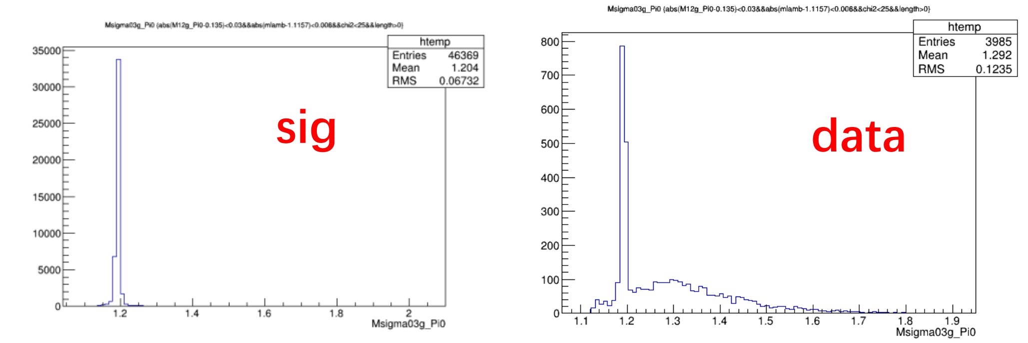


mSigma03g

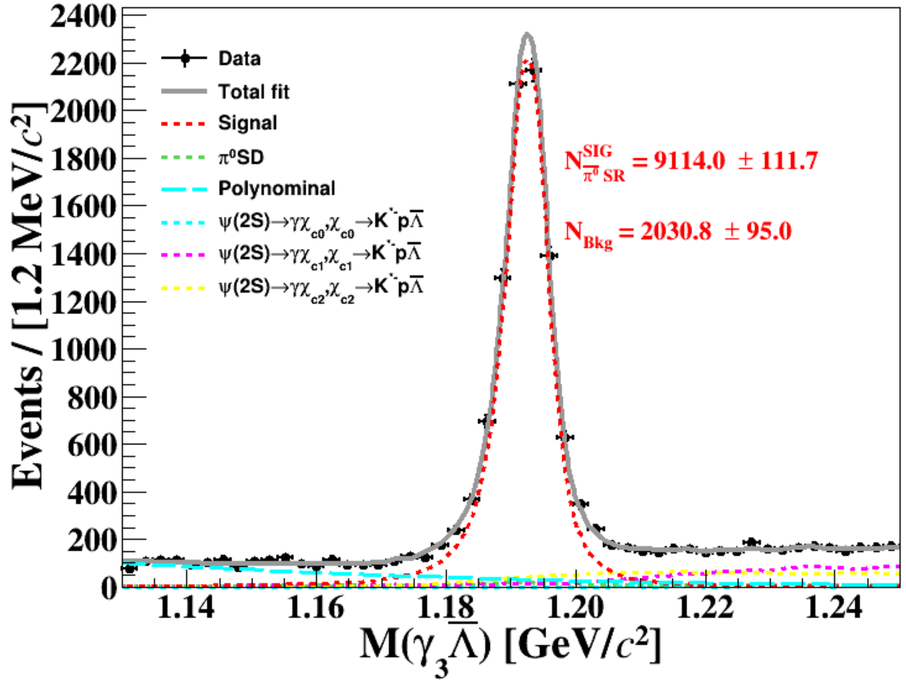


```
COVARIANCE MATRIX CALCULATED SUCCESSFULLY
FCN=-167740 FROM HESSE      STATUS=OK            62 CALLS          272 TOTAL
                     EDM=2.21737e-06    STRATEGY= 1      ERROR MATRIX ACCURATE
 EXT PARAMETER                                   INTERNAL      INTERNAL
 NO.   NAME      VALUE            ERROR          STEP SIZE       VALUE
  1  N_{chic0}    4.02122e+01   4.49429e+00   5.00000e-01  -1.43435e+01
  2  N_{chic1}    1.53000e+03   1.84117e+01   5.00000e-01  -1.56481e+00
  3  N_{chic2}    1.63002e+03   1.81659e+01   5.00000e-01  -1.52524e+00
  4  N_{sig}      9.11403e+03   1.11674e+02   2.59366e-03  -2.07441e-01
  5  NflatBkg     2.03079e+03   9.49970e+01   2.72012e-03  -9.66798e-01
  6  p0          -1.00879e+00   8.46640e-02   5.84847e-06  -3.36262e-04
  7  p1           2.45938e-01   7.12229e-02   5.36643e-06   8.19794e-05
                               ERR DEF= 0.5
```

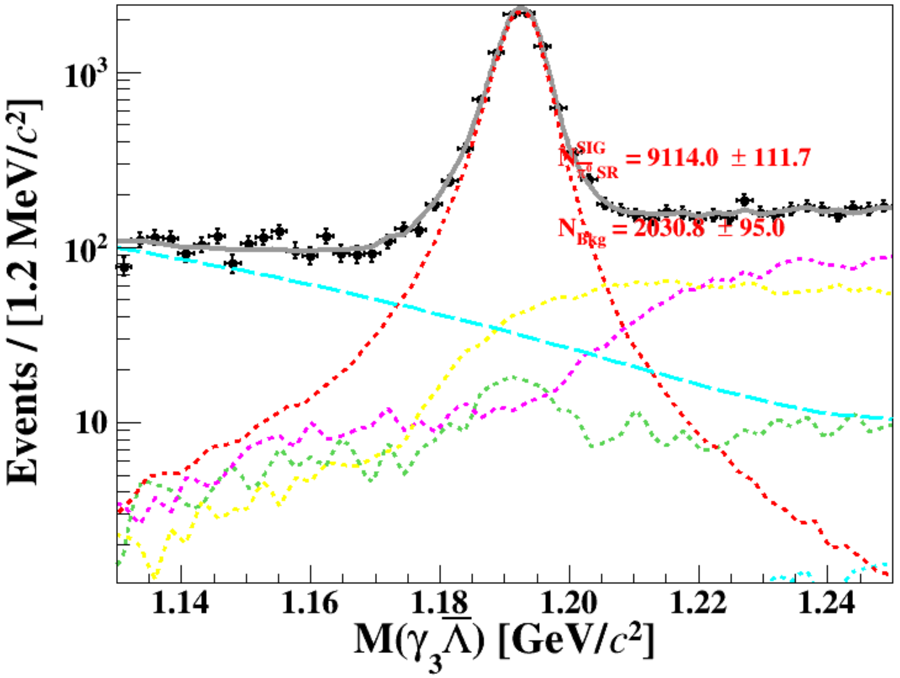


```
RooRealVar p0("p0", "poly 0",  0  ,  -3000.,  3000. );
RooRealVar p1("p1", "poly 1",   0  ,  -3000.,  3000. );//-1.4476e-03
RooRealVar p2("p2", "poly 2",  0.,  -30.,  30. );
RooRealVar p3("p3", "poly 3",  0.,  -60000.,  60000. );
RooChebychev  poly("poly","poly PDF", x, RooArgList(p0,p1));
RooPolynomial  poly("poly","poly PDF", x, RooArgList(p0,p1));


double Nmax=hh->GetEntries();

RooRealVar nsig("N_{sig}","#sig events",  0.8*Nmax, 0, Nmax);//, 0.0, 400000.0);
//      RooRealVar nchic0("N_{chic0}","#sig events",  0.1*Nmax, 0, Nmax);
        RooRealVar nchic0("N_{chic0}","#sig events",  49.22,40,60);
        RooRealVar nchic1("N_{chic1}","#sig events",  1546.12,1530,1560);
        RooRealVar nchic2("N_{chic2}","#sig events",  1646.99,1630,1660);
//      RooRealVar nchic1("N_{chic1}","#sig events",  0.1*Nmax, 0, Nmax);
//      RooRealVar nchic2("N_{chic2}","#sig events",  0.1*Nmax, 0, Nmax);
        RooRealVar Nsigma0SD("N_{sigma0SD}"," #sig events",413.5);
        RooRealVar NflatBkg ("NflatBkg "," ", 0.1*Nmax, 0, Nmax);
        //----------------------------------------------------------------
```

# Analysis II: Intermediate state (BKG Study) $\psi(3686) \to pK^-\bar{\Sigma}^0\pi^0$

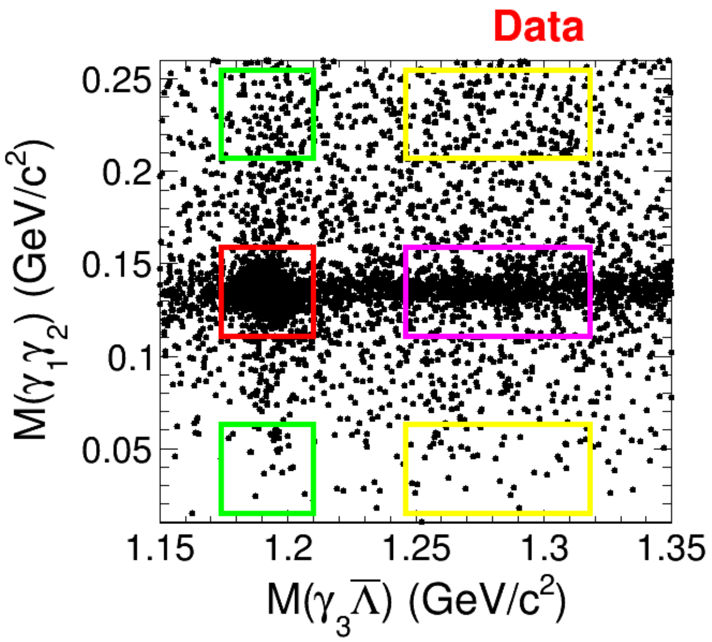


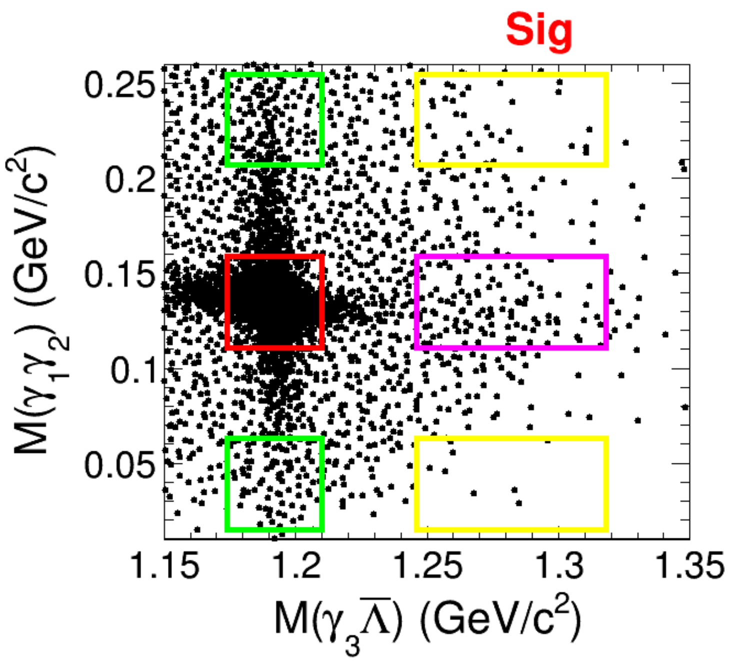


Red box:278329
Green box:833+2261
Pink box:385
Yellow box： 42+7

红色区域(*signal*)：信号
绿色区域(*sideband*$^1$)：non-$\pi^0$
粉色区域(*sideband*$^2$)：non-$\bar{\Sigma}^0$
黄色区域(*sideband*$^3$)：non- $\pi^0$,non- $\bar{\Sigma}^0$

$$N^{net} = N^{sig} - (\frac{1}{2}N_{sideband^1} + \frac{1}{2}N_{sideband^2} - \frac{1}{4}N_{sideband^3})$$

=278329-{(833+2261)/2+385/2-49/4}
=2776601.75

$\varepsilon$ =9.2%